IMPROVED KICK TOLERANCE ANALYSIS

SHINITI OHARA, SHELL BRAZIL E&P

FERNANDO FLORES-AVILA, PEMEX

edited by

JOHN ROGERS SMITH, LSU

Table of Contents

Chapter 1

Executive Summary

This LSU study was funded by the Minerals Management Services U. S. Department of the Interior, Washington, D.C., under Contract Number 14-35-001-30749. This report has not been reviewed by the Minerals Management Service and approved for publication. Approval does not signify that the contents necessarily reflect the views and policy of the Service, nor does mention of trade names or commercial products constitute endorsement or recommendation for use.

The goal of this project was to improve the basis for making kick tolerance calculations for both conventional well control and for blowouts. The specific tasks were to conduct experiments to determine the gas distribution during circulation to remove a gas kick and the critical velocity that would result in unloading of all liquid from a well during a blowout. These experiments were conducted at the LSU Petroleum Engineering Research and Technology Transfer Laboratory.

Development of an accurate kick tolerance simulator requires accurate models for estimating the upward gas rise velocity and the distribution of gas along the flow path during well control operations. These models will require a reliable basis in actual measurements of gas rise velocity and gas distributions during circulation to remove kicks. Thirty seven experiments, eight with water and twenty nine with drilling fluid, were conducted in the LSU Well No. 2 to provide these measurements. The well has a special completion that permits circulation or migration of the gas kick while being monitored with surface and downhole pressure sensors. These pressure measurements and surface rate measurements allowed calculation of both fluid velocities and average gas distributions during the experiments.

The study of the critical gas velocity to remove liquid from a well during a gas blowout was conducted using both an inclined flow loop and the LSU Well No. 1. The results from experiments performed with air and liquids, both drilling mud and water, in an experimental 48 ft flow loop at 0°, 20°, 40°, 60° and 75° deviation angles from the vertical are presented. The results show that the critical velocity that prevents control fluid accumulation can be predicted by Turner's model of terminal velocity based on the liquid droplet theory by also considering the flow regime of the continuous phase when evaluating the drag coefficient, as well as the angle of deviation from the vertical.

The results from full-scale experiments performed with natural gas and water based drilling fluid in a vertical, 2787-foot deep research well are also presented. The results confirm that the critical velocity in an actual well containing realistic fluids can also be predicted by the same adaptation of Turner's

model. The resulting model is shown to provide significantly better predictions for critical velocity than previously published models and to have practical applicability for a significant range of geometries, liquid properties, and deviation angles.

Chapter 2

Introduction

The Minerals Management Service is concerned about reducing the potential for surface and underground blowouts because Congress has mandated that MMS is responsible for worker safety and environmental protection on the outer continental shelf.

The 1994 –1999 LSU/MMS well control research project was proposed in a presentation entitled "Development of Improved Procedures for Detecting and Handling Underground Blowouts in a Marine Environment – An Overview," by A. T. Bourgoyne, Jr. and O. A. Kelly at the LSU/MMS Well Control Workshop held March 30 and 31, 1994 in Baton Rouge, Louisiana. Task PB1 of the project was proposed to consider improved methods for defining kick tolerance for avoidance of underground blowouts and was titled "Improved Kick Tolerance Analysis." The project designation was subsequently revised to be Task 7.

The goal of this project was to improve avoidance of underground blowouts by providing a more realistic assessment of the hazards associated with alternative well designs. The kick tolerance concept is a practical and quantitative basis for comparing the risk of an underground blowout for alternative designs.

Kick Tolerance

Kick tolerance is defined as the maximum underbalance, or difference between the pore pressure and mud weight in use, that can be encountered for which the resulting kick can be controlled without fracturing the weakest exposed formation. Kick tolerance is usually expressed in units of equivalent mud density. It is calculated assuming natural gas is the kick fluid. The maximum pit gain that would be expected before the blowout preventers are closed must also be assumed. The maximum pit gain used in the calculation is critical and must be selected as appropriate given existing field operating practices, rig instrumentation, and the abilities of the rig personnel.

Shut-in kick tolerance applies to well conditions when the well is shut-in. This kick tolerance can be calculated as a function of the maximum pit gain expected, given an assumed kick fluid density, the current mud weight, well depth, the fracture gradient at the weakest exposed formation, and the depth of that formation using Equation (1). The pit gain is converted to a kick length based on the annulus capacity factor. Using any set of consistent units, the kick tolerance is then the difference between the highest formation pressure gradient that can successfully be contained at shut in and the current mud density. Redman[1] gave an explanation of this calculation and its importance.

$$Kick\ Tolerance = r_f - r_m = (r_{ff} - r_m)(\frac{D_{ff}}{D}) - (r_m - r_k)(\frac{L_k}{D}) \quad (1)$$

Circulating kick tolerance applies to the most severe conditions expected during the well control operations to remove the kick fluids from the well. Redman[1] also described a method for determining a circulating kick tolerance defined as the difference between the formation pressure gradient and the equivalent circulating pressure gradient opposite the weakest exposed formation.

If the kick tolerance is exceeded during a well control operation, lost circulation is expected and could result in an underground blowout. Under certain conditions, a greater risk of an underground blowout can be tolerated if it is known that control of the well could be regained using available rig equipment. The chance of being able to regain control of the well is estimated by calculating the product of permeability, k, and permeable zone thickness, h, which could be controlled using a dynamic kill procedure and the available rig pumps. The "killable kh" is routinely calculated by some operators as drilling progresses. If it is determined that an underground blowout is not likely or that if one did occur it could be controlled with available rig equipment, a deeper casing setting depth may be selected. When the number of casing strings can be reduced, significant cost savings can be achieved without taking unacceptable risks of an underground blowout. Wessel and Tarr[2] describe a method of applying the concept of killable kh when drilling multiple objectives under variant pore pressure conditions.

Original Proposed Tasks

Based on earlier work, two areas were identified where further study was needed to improve the accuracy of the kick tolerance calculation. One area is the amount of kick dispersion that occurs in the well due to (1) bubble break-up and (2) retention of small bubbles in the mud as a function of gel strength. It is believed that a significant portion of a typical gas kick lags behind the region of high concentration as it is circulated to the surface. This increases the amount of kick dispersion, and can significantly increase kick tolerance. Additional experimental work is needed before an accurate kick tolerance simulator can be developed. In the original Subtask PB1a, experimental studies were to be conducted in the LSU No. 2 Well to provide additional data on gas-mud mixing during well control operations.

A second area where improved accuracy was needed is the determination of the critical gas rate at which mud droplets are carried from the well, reducing the liquid hold-up to zero. Application of the three methods recently presented by Gillespie et al[3] to several example well control problems has yielded a threefold spread in the computed results. In the original Subtask PB1b, experiments were to study this problem. These two subtasks made up Task PB1, which was renamed as Task 7.

Gas Distribution in Annulus

PETROBRAS had an interest in supporting research on kick tolerance analysis and sponsored one of the authors, Shiniti Ohara, to conduct experimental research to determine gas distribution in an annulus during well control operations. The results of that research are described in Chapter 3 herein and are documented in detail in a Ph.D. dissertation[4] by Ohara.

Critical Gas Velocity

Experimental research was also performed to determine a more reliable method for predicting the critical gas velocity that would completely remove liquids during a gas blowout. The second author, Fernando Flores-Avila, conducted and documented that research. He was sponsored primarily by a Fulbright Fellowship from Mexico. The experimental results and the model that was developed are described in Chapter 4. More complete documentation is included in a Ph.D. dissertation[5], and results are also explained in two professional papers by Flores, Smith, Bourgoyne, and Bourgoyne[6,7].

Additional Related LSU Research

Kick Tolerance Model

Ohara also created a computer program to predict the actual circulating kick tolerance during current operations. A description of the program was given in an LSU/MMS Well Control Workshop and is included herein as Appendix A. The program and its application are described in more detail by Ohara in his Ph.D. dissertation[4].

Liquid Hold-up During Gas Blowouts and Impact on Dynamic Kill Feasibility

Flores-Avila[5,6,7] conducted experiments in both an inclined flow tube and in an actual well to determine the liquid holdup at zero net liquid flow conditions as a function of gas rate during simulated blowouts. These measurements provide a basis for determining the impact of this liquid that remains in the well on the bottom hole pressure and therefore the flowing gas rate from the well. He and his co-researchers recently presented an additional paper[8] showing the specific application to design of dynamic kills.

Co-current and Counter-current Gas Flows in Horizontal Wells

Additional related research that was primarily funded by this MMS project focused on co-current and counter-current gas flows in near horizontal wells. The objective was to determine how hole angle, liquid flow rate, gas inflow rate, and liquid properties influenced the accumulation of gas in the near horizontal portion of a well. This accumulation of gas is important to kick tolerance because it can control how much gas enters the less deviated section of the well and therefore the length of the kick fluids that is so critical to kick tolerance.

Research by Hank Baca focused on combinations of gas and liquid superficial velocities that resulted in co-current, counter-current, or combined flows as a function of deviation angles and liquid rheologies. He studied three different rheology liquids, angles ranging from 91.5 to 100 degrees inclination, and liquid velocities typically encountered during well control operations. The results were reported in his MS thesis[9] and in two Journal of Energy Technology articles by Baca, Nikitopoulos, Smith, and Bourgoyne[10,11].

Firat Ustun extended Baca's experiments to conditions with much higher liquid superficial velocities that were more representative of conditions during routine drilling. The results were reported in his MS thesis[12].

Summary

This report will describe results of research conducted to address "Improved Kick Tolerance Analysis," which is Task 7 of the overall project on underground blowouts. The emphasis is on the two specific concerns, gas distribution in the annulus during well control and the critical gas velocity to remove all liquids from the well. These topics are addressed in Chapters 3 and 4, respectively. It also briefly summarizes related research performed at LSU in this chapter.

Nomenclature

Roman Letters

D = well depth
D_{ff} = depth to weakest zone
L_k = length of kick fluids in annulus

Greek letters

ρ_k = density of kick fluid
ρ_m = density of drilling fluid or mud
ρ_{ff} = formation fracture gradient
ρ_f = formation pressure gradient

Chapter 3

Gas Distribution in Annulus during Circulation of Kick

This chapter is based on research described in the Ph.D. dissertation by Shiniti Ohara [4]

This chapter describes experimental research to determine the distribution of gas in the annulus of a well during circulation to remove a gas kick. This work was needed to determine the upward gas rise velocity and its distribution along the flow path during well control operations for supporting more accurate determinations of kick tolerance. Thirty seven experiments, eight with water and twenty nine with drilling fluid, were conducted in the LSU Well No. 2 that has a special completion that permits simulation of a gas kick and pressure measurements in the annulus of the well. The well was monitored by surface sensors and four downhole pressure sensors.

Introduction

An effective well design and drilling plan and subsequent careful operational control to avoid kicks, loss of circulation, and underground blowouts while implementing the plan are critical to the successful drilling of most wells. An underground blowout, that can occur if returns are lost after taking a kick, can be especially costly and is highly undesirable.

The kick tolerance concept has been shown to be a powerful tool that can be used during well design, along with the pore pressure and fracture gradients, to determine casing setting depths. In addition, kick tolerance can be used while drilling to estimate the fracture risk of the weakest exposed formation, if a kick was taken and circulated, that could lead to an underground blowout. Considering this parameter, the decision to anticipate the running of casing can be made. Furthermore, it can be a parameter of interest to governmental regulatory agencies, such as the Mineral Management Service in the US for regulating drilling activities to maintain adequate safety from a well control perspective.

The circulating kick tolerance can easily be calculated as a simple model that assumes the influx of gas enters as a slug and remains as a slug during the circulation. This simple model, although easy to calculate, is very conservative if compared with a modern kick simulator as shown in Figure 1, example of a deep water well in Brazil[13].

In contrast, calculation of kick tolerance by existing kick simulators can be very time consuming. For example, it took almost one day to calculate five points to draw the upper curve in Figure 1. Although time consuming, using the kick simulators to calculate kick tolerance in this well saved

around $100,000 in drilling costs. Thus, a less conservative, more realistic, reliable, faster kick simulator dedicated to calculate kick tolerance is desirable not only for use in well planning but also while drilling.

The determination of the gas rise velocity in annuli for various wells conditions is crucial and fundamental to the development of a more accurate kick tolerance calculation procedure. Despite many studies in this area with flow loops or a real well (using mud, Xantham gum, or water as a liquid phase and air, Nitrogen, or Argon gas as a gas phase), the necessary gas distribution profile still cannot be reliably estimated. We now have some idea about the bubble front velocity, volume centered velocity, and the tail velocity, as described in the next paragraph. However, how the shape of the distribution profile will change with time during the gas migration is unknown. Since the tail velocity is low, its volume along the well can be considerable. Consequently, experiments to determine these velocities and distribution profiles have to be done.

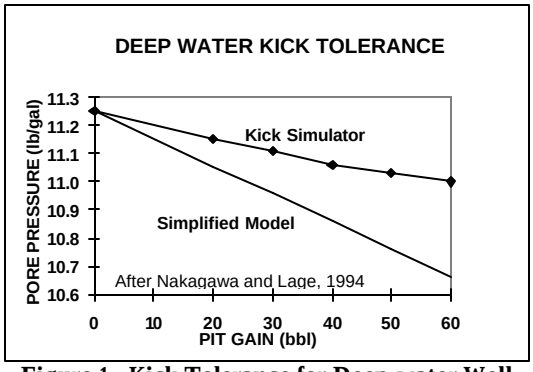

Figure 1 - Kick Tolerance for Deep-water Well

Lage et al[14] reported gas kick experiments performed in a 1,310 m (4,298 ft) vertical training well. The well has a 400 mm (13 3/8 in) casing set at 1,310 m and cemented up to surface. Inside this case, a 178 mm (7 in) casing, is placed to simulate the wellbore. A tubing of 48 mm (1.9 in) was used to inject the air at the bottom of the 178 mm casing passing through the annulus of 400 mm x 178 mm. In this same annulus an additional 48 mm tubing was placed at 800 m (2,625 ft) to simulate the casing shoe and circulation losses. Inside the 178 mm casing a drillstring composed with 121 mm (4 3/4 in) drill collars and 89 mm (3 1/2 in) drill pipes were run. A special sensor sub was made to accommodate the pressure sensor. Four sensors were placed at 302 m (991 ft), 600 m (1,968 ft), 877 m (2,877 ft), and 1,267 m (4,157 ft). Air and water were used in four tests. They measured three velocities: bubble front, volume centered, and bubble tail. If no gas is present between two sensors, the differential pressure is equal to hydrostatic pressure between them. The bubble front velocity can be measured dividing the distance between two upper sensors and the time elapsed between the beginning of differential pressure decrease in the two upper sensors and two lower sensors. Next, to measure the volume centered velocity they assumed that the center of the largest gas volume (when the differential pressure is minimum) is at the middle point of two sensors. They assumed that the air expansion and concentration changes are negligible when the volume of air rises from the center of two lower sensors to the center of the pair above. Therefore, the volume centered velocity can be measured dividing the distance between the lower and upper pair of sensors and the time elapsed between the minimum differential pressure between the lower and upper pair of sensors. The tail velocity was measured considering the distance and differential pressure stabilization between two sensors. They observed that no significant difference was obtained among the velocities for open or shut-in well conditions. They obtained an average bubble front velocity of 0.26 m/s (3,070 ft/hr), an average tail velocity of 0.09 m/s (1,063 ft/hr), and an average volume centered velocity of 0.08 m/s (944 ft/hr) to 0.15 m/s (1,772 ft/hr).

The next section will describe the experiments conducted in this project to determine actual gas distributions in an annulus during circulation of a gas kick.

Experimental Program

The procedure for determination of upward gas rise velocity and distribution factor during well control operations is presented here. This procedure was performed using a full scale well and natural gas.

Despite many studies in this area with flow loops and wells (using mud or Xantham gun as the liquid phase, and air, Nitrogen, or Argon gas as the gas phase), we have not found an experiment described in the literature that has used a full scale well with natural gas as a gas phase. During this project, thirty-seven experiments were conducted, eight with water and twenty nine with drilling mud.

Description of a full-scale well: LSU No. 2

The experiments were carried out in the existing LSU Well No. 2, located at the Blowout Prevention Research Well Facility in Baton Rouge, Louisiana. The LSU Well No. 2 is a vertical well which is 1,793 m (5,884 ft) deep and cased with 244 mm (9 5/8 in) casing. The well is completed with a 32 mm (1 1/4 in) gas injection line run concentrically in a 89 mm (3 1/2 in) drilling fluid injection line. The well also contains 60 mm (2 3/8 in) perforated tubing which serves as a guide for well logging tools to be run in the annulus without risk of the logging cable wrapping around the drill string and becoming stuck.

Methodology of experiments

Drilling fluid compositions similar to those utilized to drill deep-water wells in the Campos Basin, offshore of Brazil, and natural gas was utilized. Fluid densities of 9.6 to 10.0 lb/gal were used. These fluids had plastic viscosities ranging from 10 to 30 cp, and yield points from 5 to 15 lbs/100sf.

The gas was injected at the desired injection rate through the 32 mm (1 1/4 in) tubing. Drilling fluid was circulated down the annulus between the 89 mm (3 1/2 in) and 32 mm (1 1/4 in) tubings at the desired mud flow rate with returns taken from the 244 mm (9 5/8 in) casing.

During the experiments the drill pipe, casing and gas-injection pressures at the surface were continuously monitored. The mud rate and the gas rate into and out of the well were also measured. One wired-to-surface downhole pressure sensor and three downhole pressure recording sensors monitored the pressures developed during the well control experiments. A pressure signal generated at the beginning of the experiment was used to synchronize all four sensors in time. To investigate the concentration of gas in the tail of the multiphase region, a gas detector was used at the shale shaker to indicate the gas concentration present in the mud.

Methodology to measure gas rise velocities

The velocity of the kick front, velocity of the peak gas concentration, and the velocity of the tail of the two-phase region, see Figure 2, were estimated through an analysis of the measured differential pressures. If no gas is present between two consecutive pressure sensors and mud is not being circulated, the differential pressure should reflect the hydrostatic pressure between them. When mud

is being circulated, the differential pressure between two sensors should be equal to the sum of the hydrostatic pressure and the pressure losses between them.

When the gas front reaches each sensor, the differential pressure begins to decrease denoting the arrival of the bubble front. Thus, the velocity of the front can be estimated by dividing the distance between sensors by the elapsed time between the first arrival of the front. For example, from the Figure 3, the bubble front velocity between sensors 3 and 4 can be estimated knowing the distance $d_{3,4}$ and the time elapsed between the observed initial decrease in differential pressure between sensors 2,3 and sensors 3,4 using the following equation:

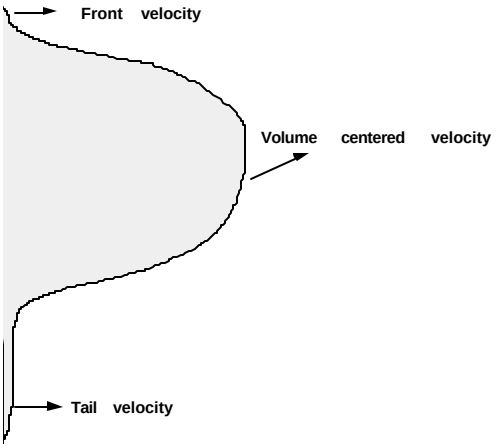

Figure 2 - Conceptual Gas Distribution Profile

$$v_{front} = \frac{d_{3,4}}{\left(t_{2,3ini\Delta p} - t_{3,4ini\Delta p}\right)} \qquad (2)$$

Similarly, the tail velocity can be calculated as the distance between two sensors (for example, sensor 2 and 3) divided by the elapsed time to stabilize two adjacent differential pressures.

$$v_{tail} = \frac{d_{2,3}}{\left(t_{3,4\,stab\Delta p} - t_{2,3stab\Delta p}\right)} \qquad (3)$$

When the differential pressure between two sensors is a minimum, the largest amount of gas is present between the sensors, but the exact position of the peak concentration is not known. If it is assumed that the peak concentration occurs at the mid-point between two sensors, then the velocity of peak concentration can be computed as the distance between two mid points (e.g. between mid-point of sensors 3 and 4, and mid-point of sensors 2 and 3) divided by the elapsed time between them when the minimum values of differential pressure were recorded in the two adjacent well segments

$$v_{center} = \frac{\frac{d_{3,4}}{2} - \frac{d_{2,3}}{2}}{t_{4,3_{\min \Delta p}} - t_{2,3_{\min \Delta p}}} \qquad (4)$$

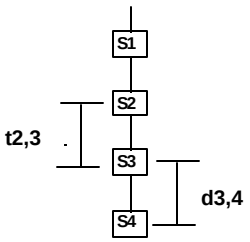

Figure 3 - Position of Downhole Pressure Sensors

After eight experiments with water and gas, twenty nine experiments were performed with drilling fluid and natural gas. The main parameters varied in the experiments were gas injection rate, pit gain volume, mud circulation rate, drilling fluid yield point and plastic viscosity, and the pressure sensor positions.

Gas Distribution Profile

The gas fraction in a depth interval between two pressure sensors was calculated as a function of time based on the pressure difference between the two sensors. Knowledge of the gas fraction in each depth interval versus time allowed the gas distribution in the entire wellbore to be estimated at any point in time. Using the experimental data, we could therefore determine how the gas distribution profile along the well changes with time during the circulation of a kick. This allows

comparison of actual results to the simple assumption typically used in determining kick tolerance that the gas remains in a single slug. If the tail velocity is low compared with the leading edge velocity or front velocity, as is expected, the gas volume may actually be distributed over a significant length in the well. Consequently, the simple slug assumption for determining kick tolerance may be overly conservative as implied by comprehensive well control simulators.

Experimental Results

The twenty nine tests conducted with drilling fluid and natural gas in the LSU Well No. 2 were analyzed to determine gas velocities and distribution. The drill pipe, casing and gas-injection pressures at the surface, the mud rate in, the gas rate in, the gas rate out, the pit volume, and a wired-to-surface downhole pressure were recorded in a LabView® data file. The three subsurface pressures recorded downhole were downloaded into separate files. All four files were combined by using the pressure pike generated at the beginning of an experiment to synchronize all four files in time. More detailed descriptions of the well, methodology, instrumentation, and results are provided in the dissertation[4] by this author (Ohara).

Typical data collected during an experiment are shown in Figures 4, 5, and 6. The data shown are from Experiment M9 in which the gas kick was injected into the well at 82 spm, or a velocity of 1.64 ft/sec, and then circulated out at a rate of 32 spm, or a superficial liquid velocity of .64 ft/sec, with a choke pressure of 160 to 180 psig. The pressure differential between two adjacent sensors was then used to calculate the gas rise velocity over the depth interval between the sensors. An example of the pressure differentials versus time is shown for this same experiment in Figure 7. The upper figure is the differential between the upper most sensor, which was the on-line sensor, and the casing pressure. Note that the maximum pressure differential occurs first between the bottom and middle sensors and then moves up in time as the gas is circulated out of the well.

These pressure differentials were then used to calculate the leading edge velocities. These velocities were then plotted versus mixture velocity on the Zuber-Findlay[15] plot shown in Figure 8.

This data was also plotted with previous experimental data by published by Johnson and White[16], Nakagawa[17], Mendes[18], and Wang[19]. The composite plot is shown as Figure 9. All of the data lies on approximately the same trend allowing an empirical model of gas velocity versus mixture velocity to be defined. This model is

$$v_g = 1.426\, v_{mix} + 0.2125 \tag{5}$$

The differential pressure data was also used to estimate the void, or gas, fraction in the depth interval between two sensors as described in the previous section. As the gas fraction increases in a particular depth interval, the differential pressure decreases until the gas fraction reaches a maximum and then increases as the gas leaves the interval. The gas fraction, α, in the interval can be approximated at a given time, *t*, with the following equation.

$$a(t) = 1 - \left[\frac{p_{bottom}(t) - p_{top}(t)}{\Delta p_{\max}} \right] \qquad (6)$$

The actual pressure difference is compared to the maximum pressure difference measured over the interval at the same pump rate, Δp_{max}, and the reduction is assumed to be due to the reduction in hydrostatic due to a zero density gas. Figure 10 shows the calculated values for gas fraction versus time from Experiment M9. The calculated gas fraction for a given interval at a given time was then combined with data from the other intervals at the same time to develop a gas distribution in the wellbore versus depth at a given time. Example distributions from Experiment M9 are shown in Figure 11. Although these distributions were the ultimate goal of these experiments, the gas fraction is only calculated as an average over each of four long intervals. Therefore the calculated distributions are coarse estimates of the actual distribution.

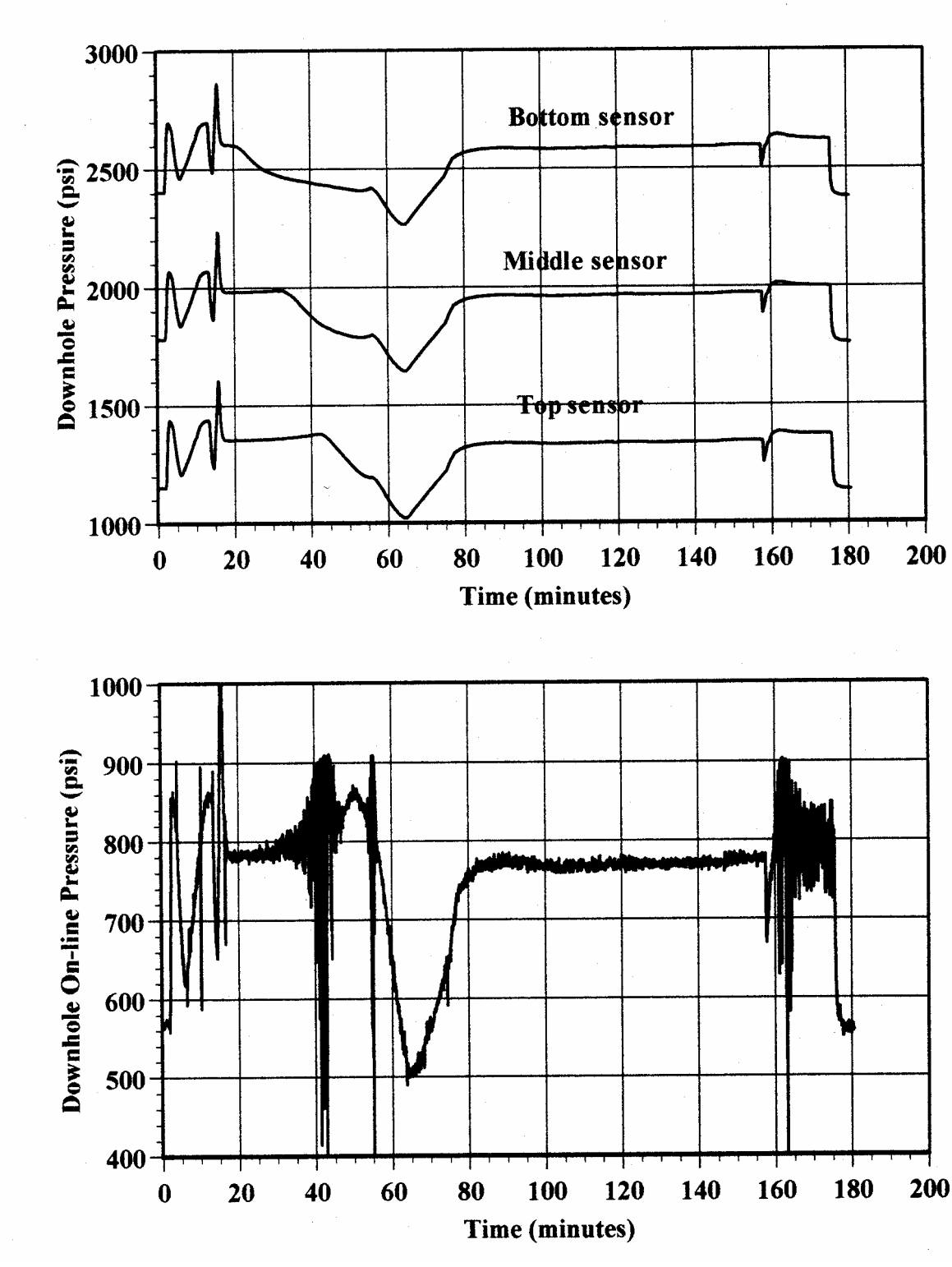

Figure 4 - Example Downhole Pressure Data

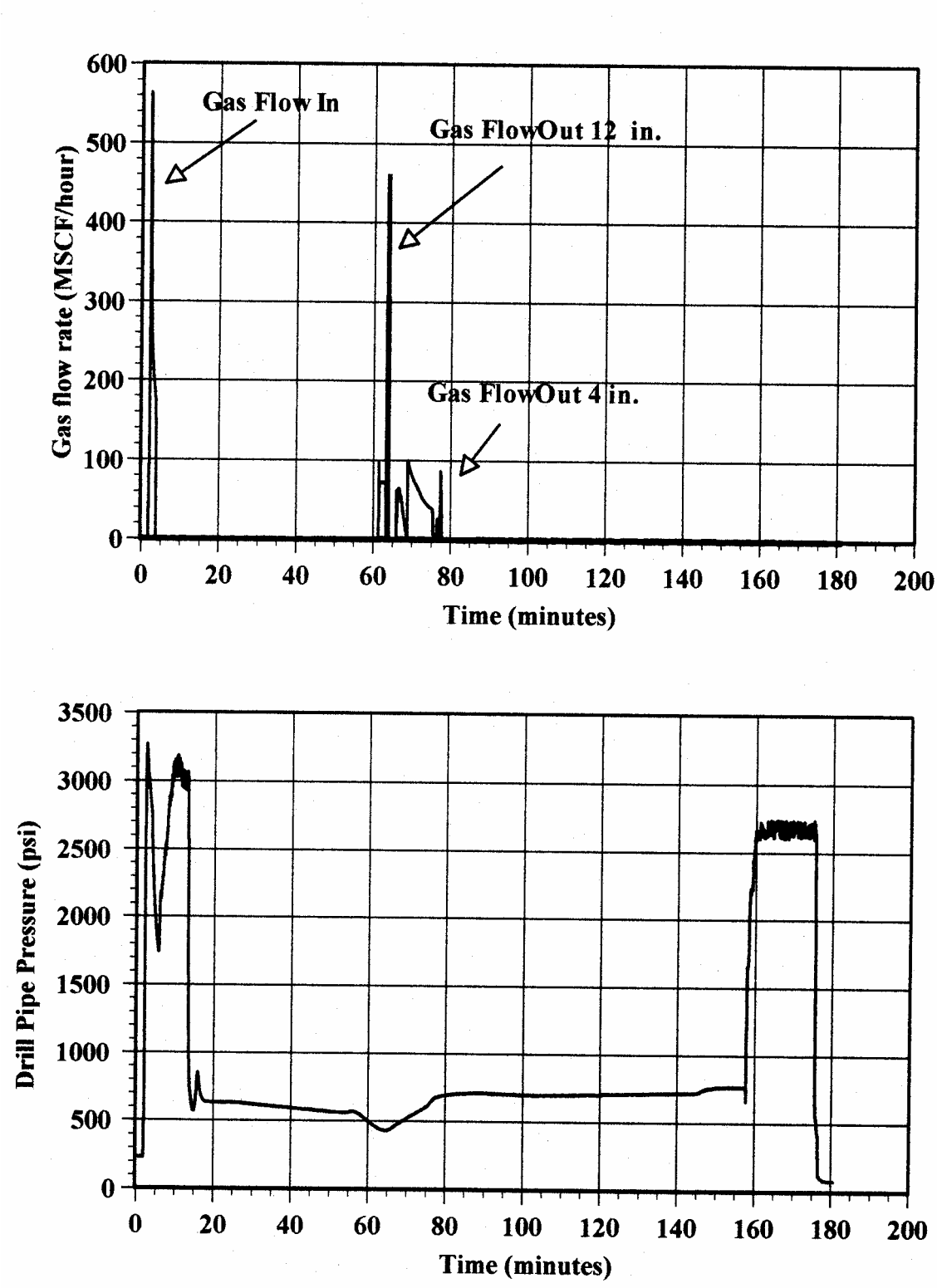

Figure 5 - Example of Gas Flow Rates and Drill Pipe Pressure

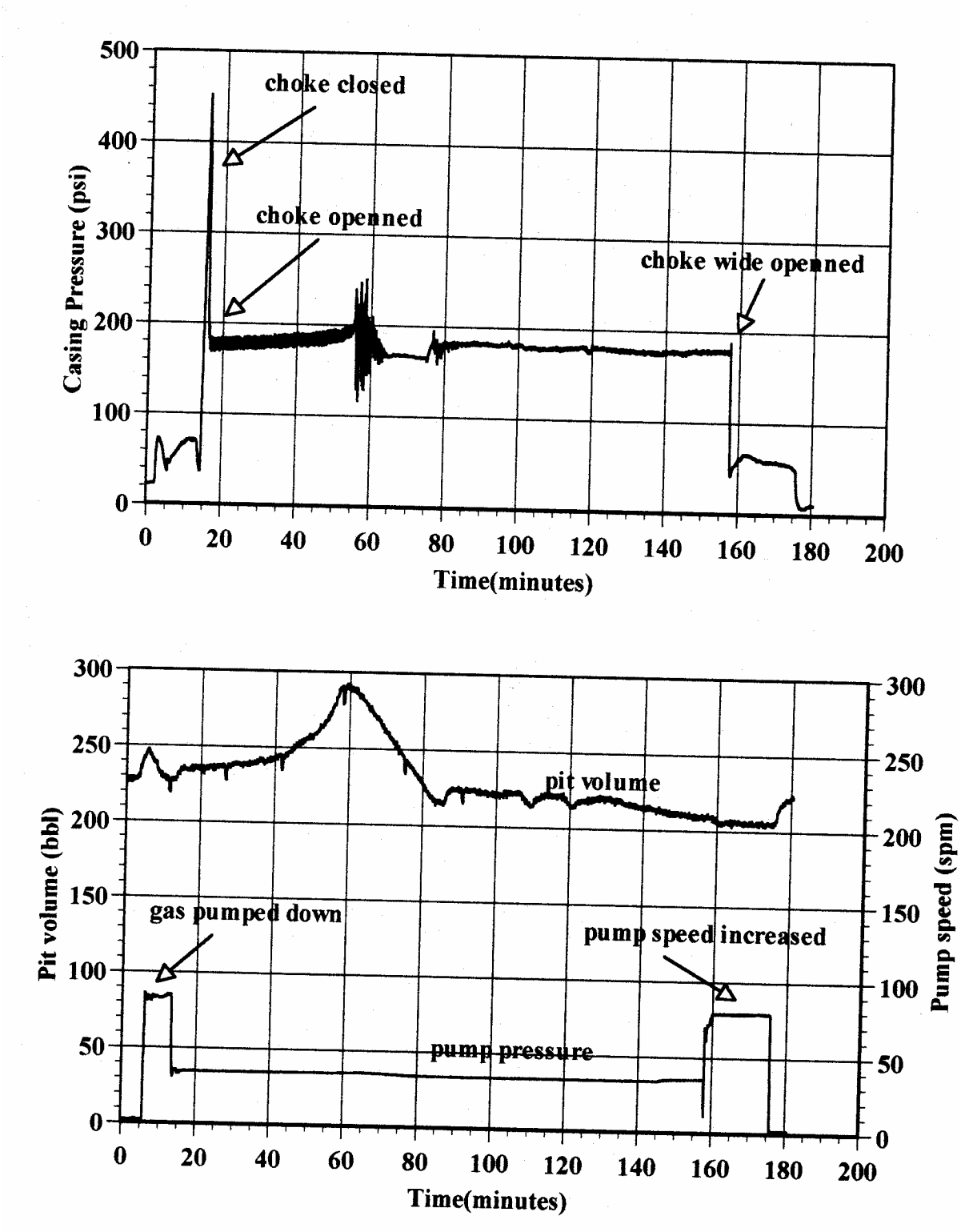

Figure 6 – Example of Casing Pressure, Pit Volume, and Pump Speed (not pump pressure)

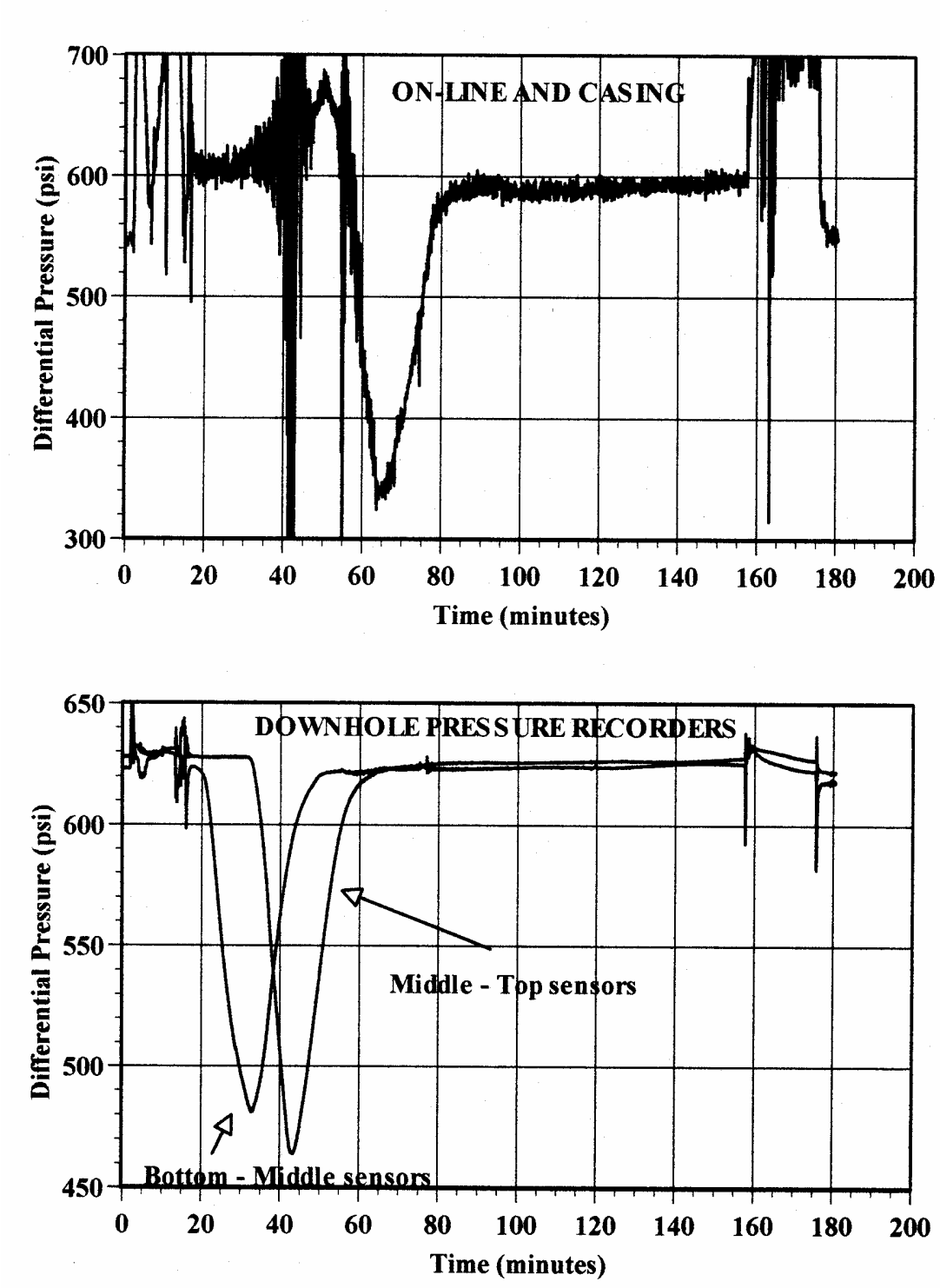

Figure 7 - Example Differential Pressures versus Time

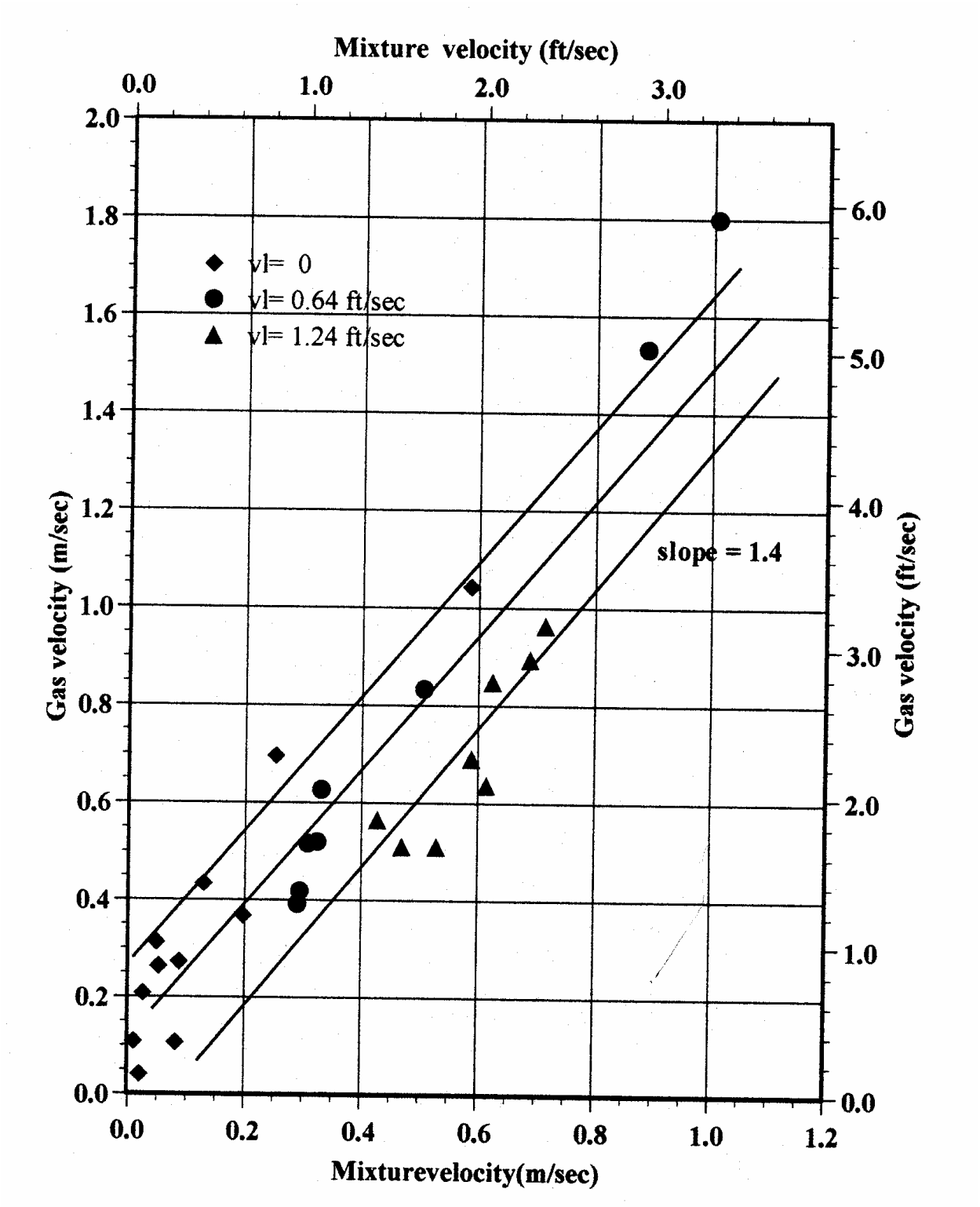

Figure 8 – Zuber-Findlay Plot of Experimental Data

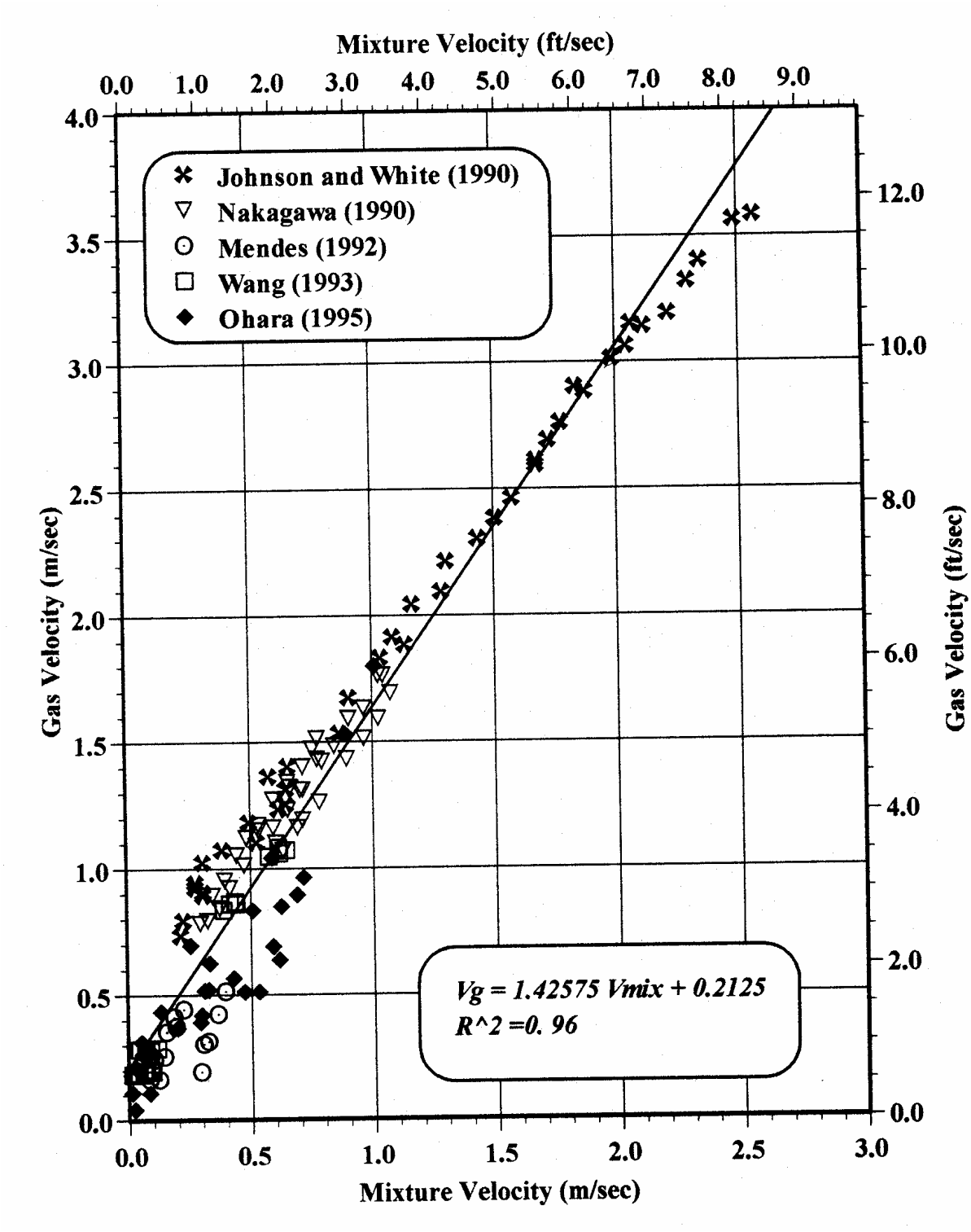

Figure 9 – Zuber-Findlay Plot of Current Well and Previous Flow Loop Data

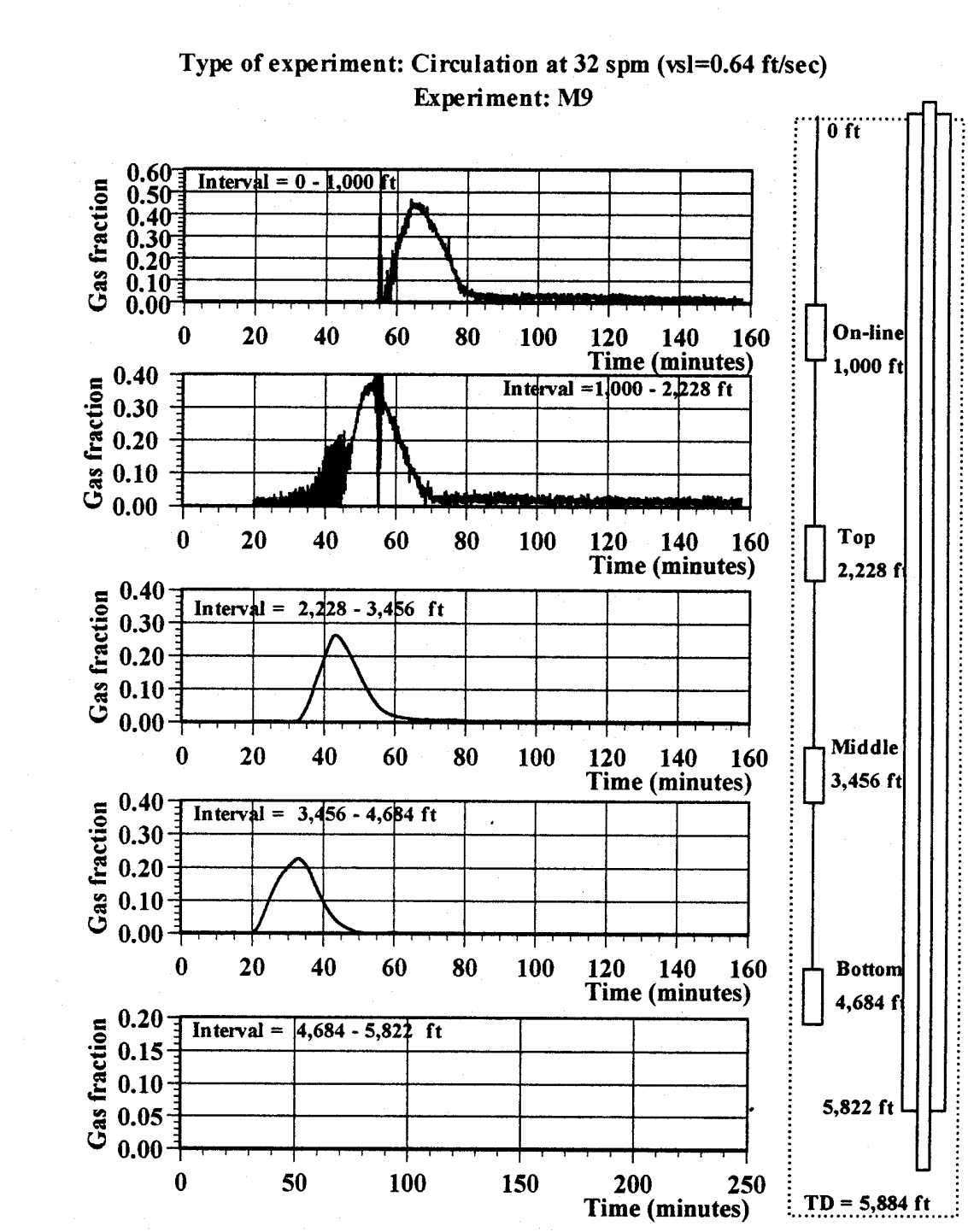

Figure 10 – Gas Fraction for Depth Intervals versus Time for Experiment M9

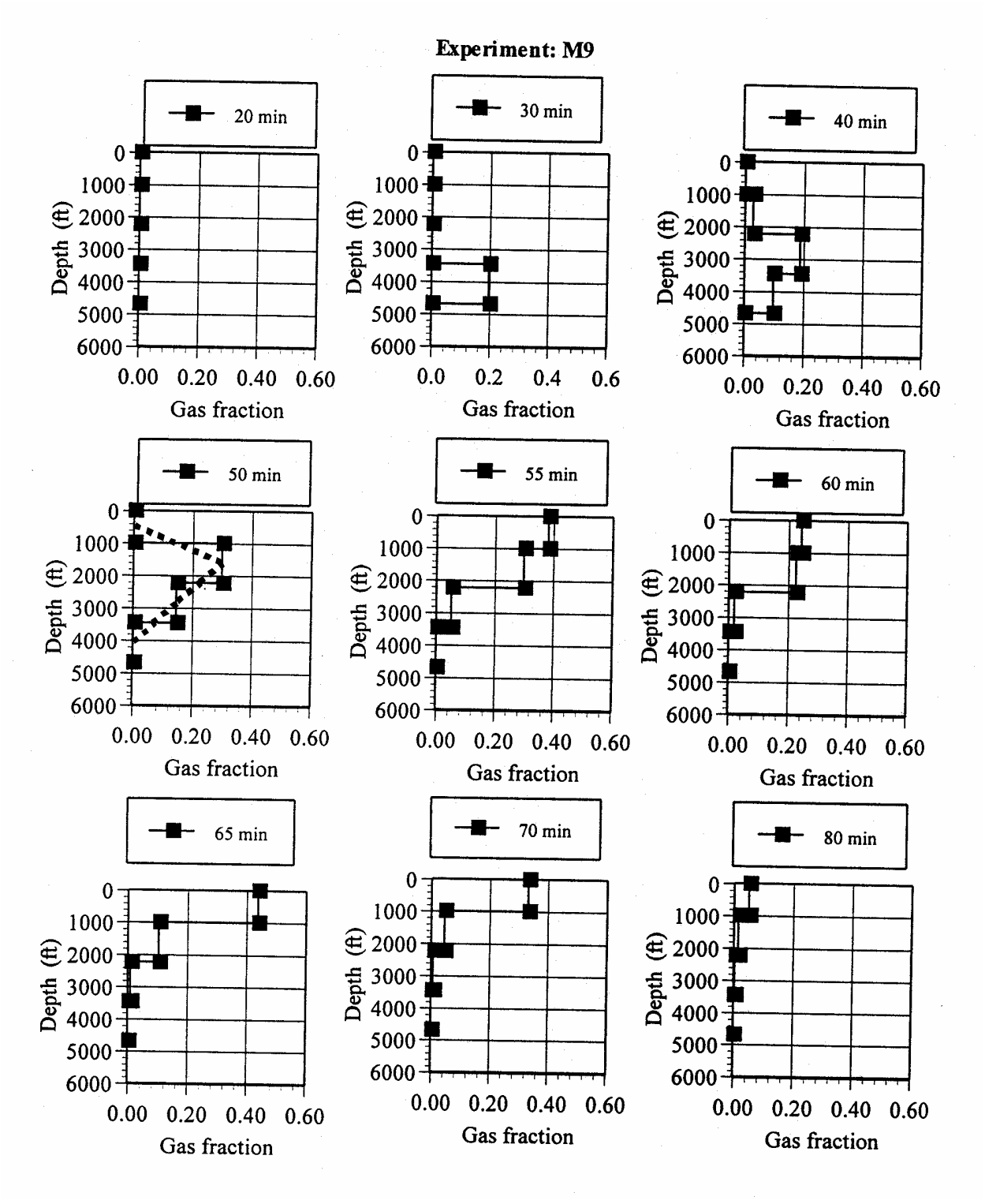

Figure 11 – Gas Fraction versus Depth at Selected Times for Experiment M9

Equivalent results for Experiments M1 and M8 are given in Figures 12 through 15. Experiment M1 was conducted at a higher circulating rate of 62 spm for a superficial liquid velocity of about 1.24 ft/sec with a choke pressure of approximately 170 psig. Figure 13 shows that the gas reached the surface after about the same amount of time as in Experiment M9 even though the liquid velocity was much higher. However, it appears that the gas was removed more in the form of a single, high void ratio slug than in M9. Nevertheless, there was still a tail of trailing gas concentration after the main slug of gas was removed. Also, the gas fraction calculations for the top two intervals, especially from 0 to 1000 ft, do not appear to be reliable. Consequently, strong conclusions about when the gas reached the surface and what gas concentrations were near the surface were not possible.

Experiment M8 was conducted with the choke open and no circulation. Consequently, it was a test of freely migrating and expanding natural gas. The gas front in this case also reached the surface quickly, but not as rapidly as when being circulated up. In addition, the void fractions were very high, up to 60%, as the gas approached the surface and expanded, presumably due to the choke pressure being lower than in the other two examples. In this case, a void fraction remained at the surface after most of the gas had exited the well due to the loss of liquid that was unloaded by the gas flow and not replaced.

Data from the remaining twenty six tests with drilling fluid are included in the dissertation[4] by the author (Ohara). Tests were conducted with different viscosity drilling fluids, and different gas kick sizes, as well as the varied mud pump rates and surface pressures. In addition, some tests were conducted with different pressure sensor placement in order to get higher resolution in determining void fraction versus depth.

The dashed lines on the 50 minute plot in Figure 11 connects the average gas concentrations, void fractions, plotted at the center of each interval. This interpretation of the data provides a potentially more realistic distribution of the gas in the annulus because it assumes a more continuous distribution than the base plots. The base plots show the average concentration in an interval as occurring and being constant throughout the interval. This results in step changes in the concentration, which are unlikely in reality.

The triangular shape of the gas distribution versus depth portrayed by the dashed lines in Figure 11 was observed over a range of time in a number of the tests. A tentative, conceptual model describing a triangular gas distribution was proposed in the dissertation[4]. It was based on knowing the gas front and the gas volume, and estimating the velocity of the gas tail as the liquid velocity.

A full study of these gas distribution profiles and development of a gas distribution model was not possible because of the time constraint on the author.

Note: Continued following figures

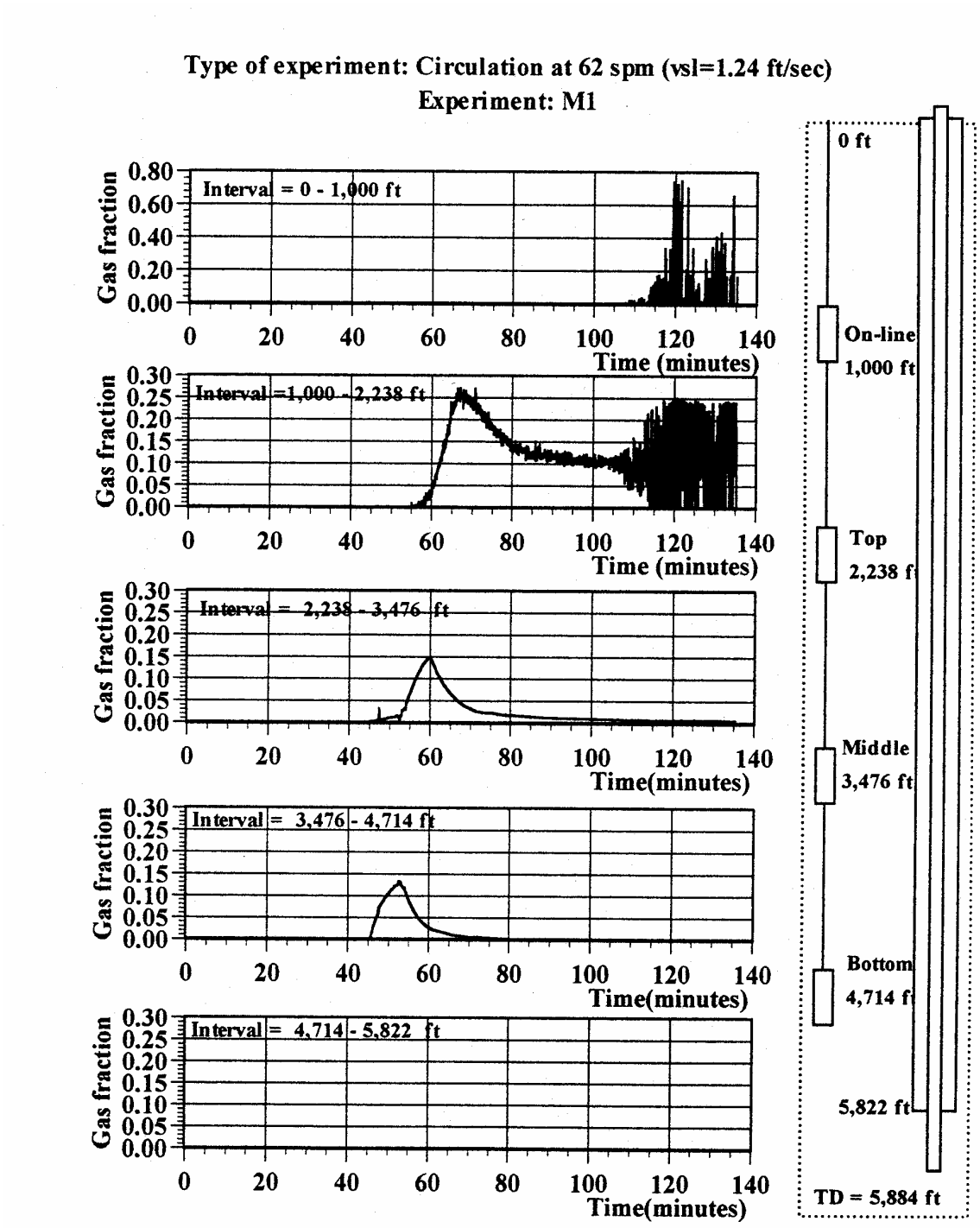

Figure 12 – Gas Fraction Data from Experiment M1

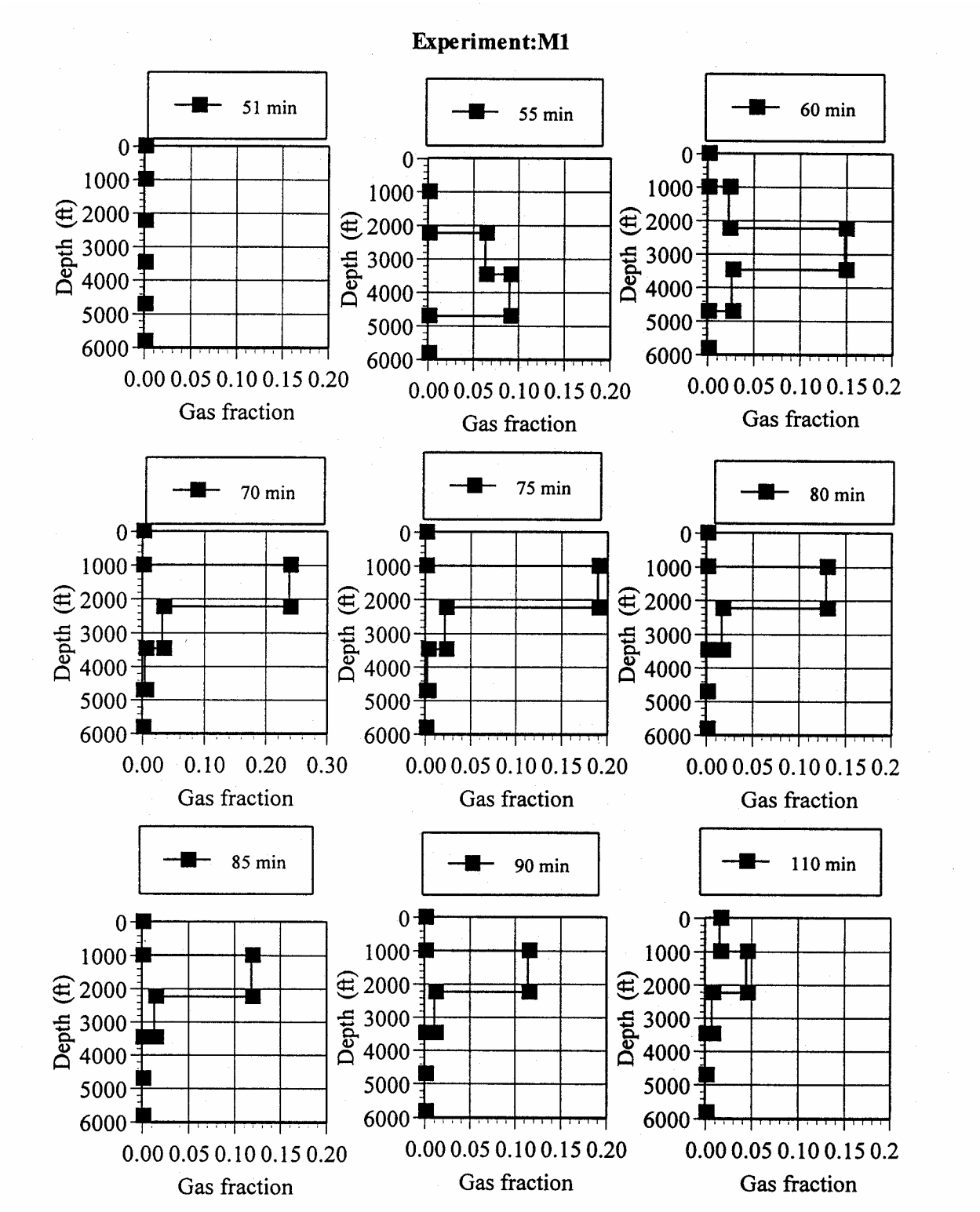

Figure 13 - Gas Fraction versus Depth at Selected Times for Experiment M1

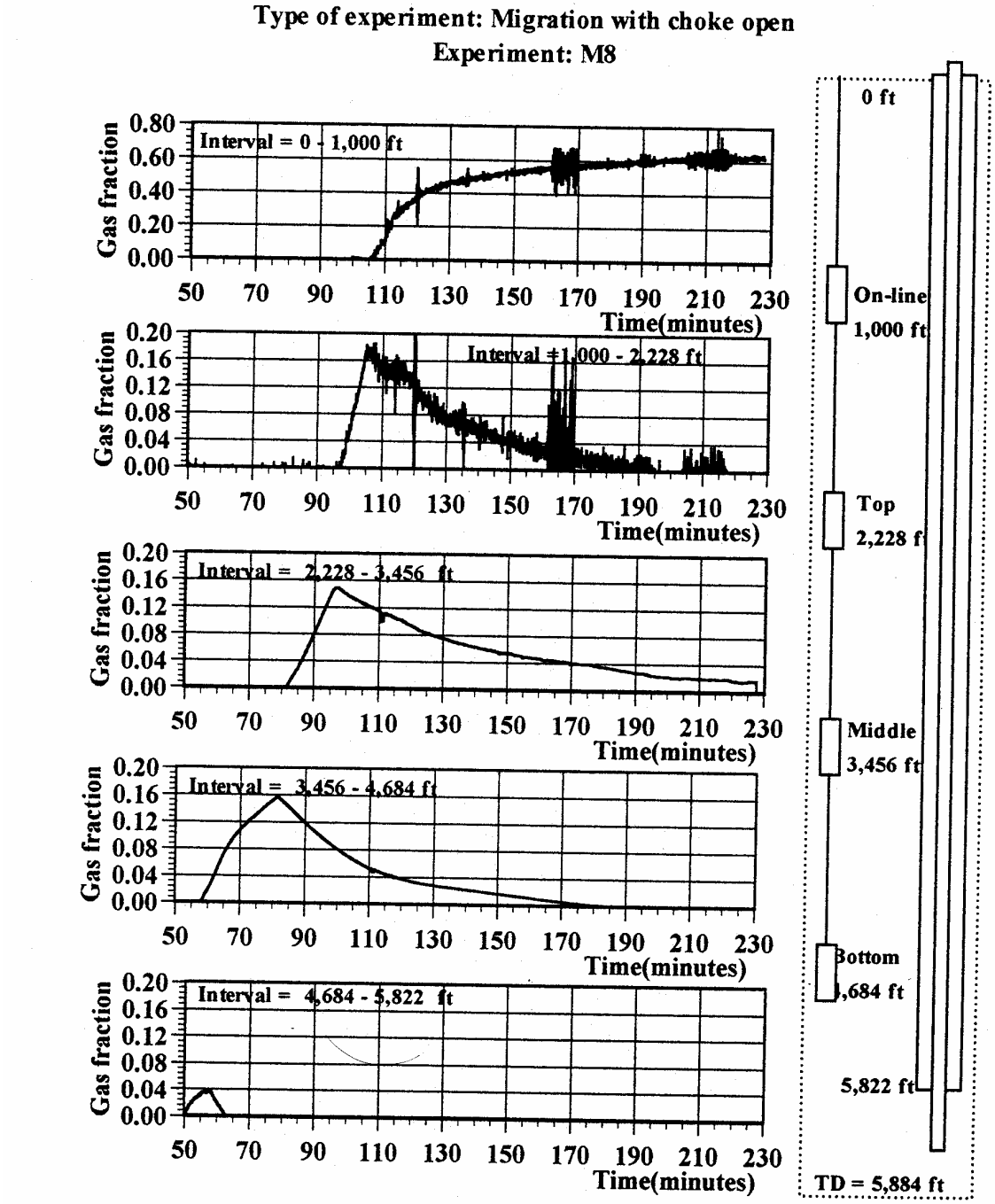

Figure 14 – Gas Fraction Data from Experiment M8

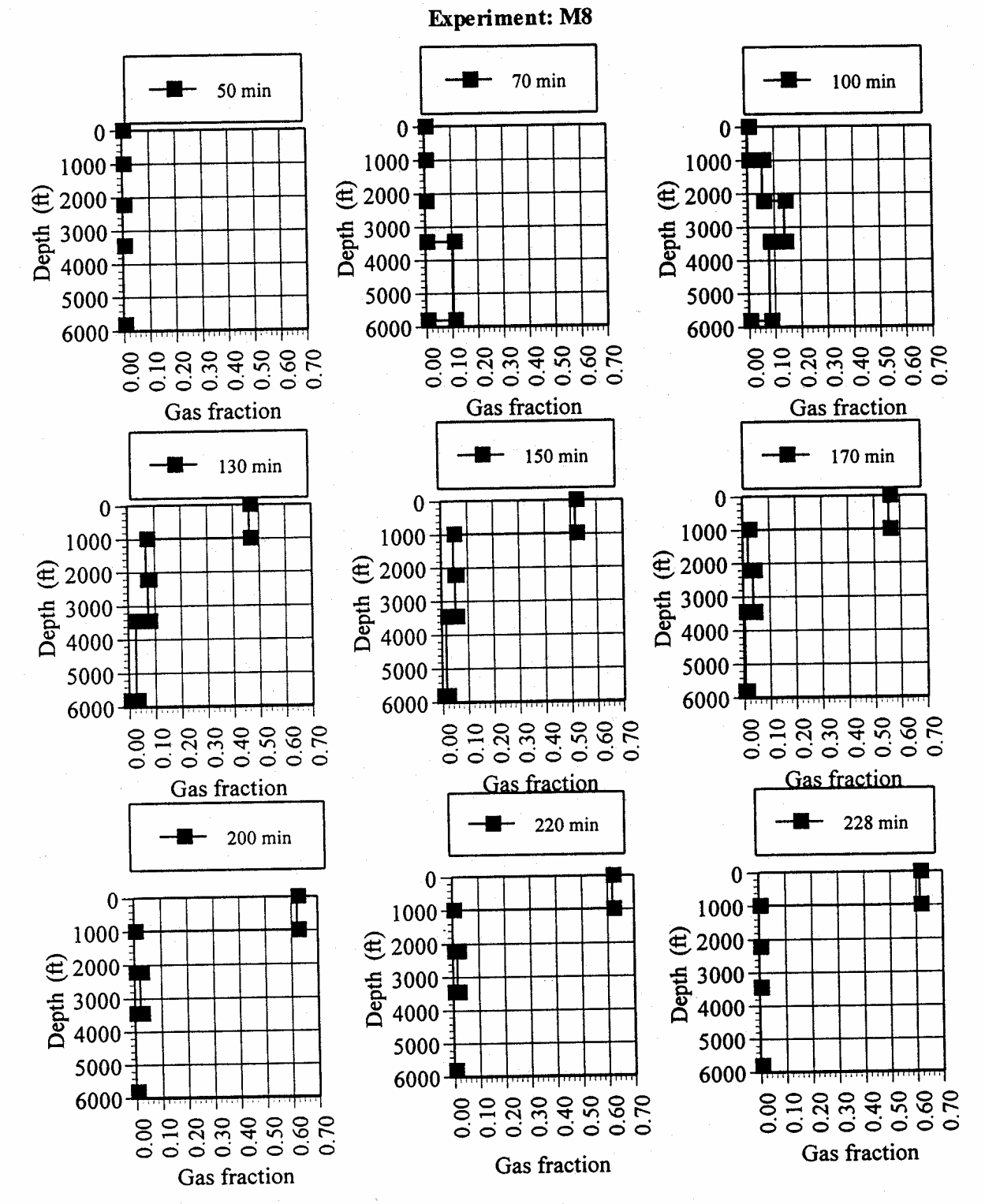

Figure 15 - Gas Fraction versus Depth at Selected Times for Experiment M8

Conclusions

1. Results of gas rise velocity obtained by previous researchers using flow tube data and the full scale experiments conducted as a part of this research are in close agreement.

2. Based on the experimental results, a simplified triangular gas distribution profile along the upward migration of the gas would be expected to provide further improvement in the accuracy of kick tolerance calculations.

Nomenclature

Roman Letters

d = distance
p = pressure
t = time
v_{center} = volume centered gas velocity
v_{front} = gas front velocity
v_g = mean gas velocity
v_{mix} = mixture or homogeneous velocity
v_{tail} = gas tail velocity

Greek letters

α = void (gas) fraction

Chapter 4

Critical Gas Velocity to Unload Liquid During a Gas Blowout

This chapter is based on research described in the Ph.D. dissertation by Fernando Flores-Avila[5].

This section deals with the determination of the critical gas rate at which mud droplets are carried from the well, reducing the liquid hold-up to zero. Application of the three methods recently presented by Gillespie et al[3] to several example well control problems has yielded a threefold spread in the computed results. The experiments conducted for this section allowed development of a definitive, semi-mechanistic model that provides a reliable estimate of critical gas velocity for a significant range of hole angle, annulus geometries, and fluid properties. A more detailed explanation of the experiments, the results, and the evaluation of the proposed model for critical velocity is available in the dissertation[5] by the author (Flores-Avila).

Introduction

Despite success from improved technology and training, blowouts and underground blowouts still happen. One cause of these occurrences is taking a kick that exceeds the kick tolerance. This results in lost returns which can evolve to an underground blowout and then potentially to a surface blowout.

The liquid holdup that remains in a well during a developing or a full-fledged blowout has a significant impact on the bottomhole pressure and therefore the formation fluid flow rate from the well. In addition, the ability to predict whether control fluids will fall and accumulate in a well can be important in determining whether it can be controlled or killed. Knowing the critical velocity that would remove all liquid from a blowout is therefore an important consideration in determining whether a kick that would exceed the kick tolerance is killable using the rig equipment.

Background

The first study considering the countercurrent flow of kill fluid falling through formation fluid was conducted and published by Gillespie et al[3]. They considered the application of the dynamic kill principle to an off bottom scenario in a vertical well, during a workover, that considered the beneficial effect of such fallback on the potential for achieving a successful kill.

Gillespie et al[3] provided a method for estimating the conditions at which liquid would begin to fall through the gas by estimating the critical gas velocity at which liquid would no longer fall. However, no means for estimating the liquid holdup that would exist at a given injection rate was provided. They pointed out that the mechanism of breakup of the liquid into droplets is a complex process controlled by aerodynamic and hydrodynamic effects. They also mentioned that a conservative estimate of those conditions leading to a well kill could be obtained by determining two factors: the largest diameter of droplet likely to exist in the gas stream and a conservative value for the drag coefficient of the droplet.

They presented three different methods to estimate the maximum likely droplet size. The first was based on work developed by Hinze[20] and Hanson et al [21] as shown in Equation (7):

$$d_{\max} = \frac{20s}{r_c v_s^2} \quad \text{.....(7)}$$

The second was based on the model developed by Karabelas[22] who considered a liquid-liquid dispersion system as shown in Equation (8):

$$d_{\max} \approx d_{95} = \frac{4d_i}{\left(d_i r_c \bar{v}^2 / s\right)^{0.6}} \text{.....(8)}$$

The third method they proposed was based in Sleicher's[23] work, also considered a system of two liquids. His expression to estimate the maximum droplet diameter is shown in Equation (9):

$$d_{\max} = 38 \frac{s}{r_c \bar{v}^2} \sqrt{\frac{g_c s}{m_c \bar{v}}} \left[1 + 0.7 \left(\frac{m_d \bar{v}}{g_c s}\right)^{0.7}\right] \text{.....(9)}$$

The critical gas velocity is defined as the velocity at which liquid droplets would just begin to fall. It is assumed to be equal to the relative settling slip velocity of the maximum size droplet. Gillespie et al[3] proposed that this critical velocity v_{Scrit} is given by Equation (10):

$$v_{Scrit} = \sqrt{\frac{4gd_{\max}\left(r_d - r_c\right)}{3r_c K_d}} \text{.....(10)}$$

They also stated that the drag coefficient, K_d is a function of the Reynolds number, N_{Re}, based on the slip velocity (velocity of the droplet relative to the moving gas stream) as shown in Equation (11):

$$N_{\mathrm{Re}} = \frac{d_{\max}\, r_c\, v_s}{m_c} \quad \text{.....(11)}$$

They proposed using a maximum likely value for the drag coefficient, because a smaller value would result in a lower, less conservative estimate of a v_{Scrit}. Equation (12) was proposed for giving a conservative estimate of the drag coefficient based on quiescent fluid and neglecting the sudden drop in value of drag coefficient associated with reaching the critical Reynolds number.

$$K_d = F\left[\frac{24}{N_{\mathrm{Re}}} + \frac{4}{N_{\mathrm{Re}}^{0.468}} + 0.5\right] \quad \text{.....(12)}$$

They proposed to use the value of F=4 in Equation (12) based on the work done by Lopez et al[24] and others. However, Gillespie et al[3] and Lopez et al[24] further indicate that the drag coefficient is dependent on the gas-turbulence intensity level.

Gillespie et al[3] then estimated the critical gas flow rate, for the specific case they were analyzing, using the three different approaches in droplet size given by Equations (7), (8) and (9). For their specific case, the maximum flow rate calculated was almost four times the minimum rate calculated. This means that there is a large of discrepancy between the three methods evaluated.

Turner et al[25] developed an equation to calculate the critical gas velocity to predict when a gas well will load-up. They compared two physical models for transporting fluids up vertical conduits: liquid film movement along the pipe walls and liquid droplets entrained in the high velocity gas core. A comparison of these two models with field test data yielded the conclusion that the onset of load-up could be predicted adequately with Equation (13), which considers a 20% upward adjustment from the theoretical expression developed.

$$v_{Scrit} = 20.4\frac{s^{1/4}\left(r_L - r_g\right)^{1/4}}{r_g^{1/2}} \quad \text{.....(13)}$$

Kouba et al[26] presented a method for quantifying the volume fraction of kill fluid below the point of injection in an off bottom dynamic kill situation in a vertical well. They also proposed expressions to calculate formation flow rate below which liquid holdup will occur. He based his work on a flow-pattern map based on the Taitel et al[27] mechanistic model. The transition boundary between annular and non-annular flow was developed from a force balance on a droplet of liquid in a gas stream. The minimum velocity required to suspend a liquid droplet marks this transition and is given by Equation (14), where σ is in dyne/cm:

$$v_{Scrit} = 1.593\left[\frac{s\left(r_L - r_g\right)}{r_g^2}\right]^{1/4} \quad \text{.....(14)}$$

This equation is the one proposed originally by Turner et al[25] without the 20% upward adjustment he proposed, and was shown to provide good results by Coleman et al[28]. They satisfactorily tested this expression in a study that determined when low-pressure gas wells would begin liquid loading. Kouba rewrote Equation (14) in terms of standard volumetric flow rate as shown in Equation (15). Below this flow rate, injected liquid will begin to fall downward, partially flooding the region below the point of injection:

$$q_{gsc} = 4.87 \frac{A_p p}{z_{\bar{p}} T} \left[\frac{\sigma(\rho_L - \rho_g)}{\rho_g^2} \right]^{1/4} \quad \text{.....(15)}$$

New Proposed Method

The critical velocity for complete liquid removal used herein is based on the terminal velocity and the liquid droplet theory. The original expression presented by Turner et al[25] is adapted to the units used herein and to consider the deviation angle from the vertical (α), as shown in Equation (16):

$$v_{Scrit} = 14.27 \left[\frac{s\left(r_L - r_g\right)}{K_d \cos a \; r_g^2} \right]^{1/4} \quad \text{.....(16)}$$

The drag coefficient K_d that corresponds to the Reynolds Number at the flowing conditions of the continuous phase should be used in Equation (16) as suggested by Nosseir et al[29]. The diameter used in Equation (11) for calculating the Reynolds number, is the equivalent circular diameter, equal to four times the hydraulic radius for an annular flow geometry, and equal to the pipe internal diameter in our tubing flow geometry. This criteria was selected because the flow regime around the droplet is expected to be turbulent or highly turbulent due to the high gas velocities regardless of the droplet size. An iterative process is required because the critical velocity is needed to calculate the Reynolds number. It is recommended to use K_d =0.44 for the first iteration to calculate the first critical velocity, and then a new K_d read from Figure 16 for a sphere using the new Reynolds number calculated. Normally at blowout conditions, the Reynolds number reached is in the highly turbulent region, resulting in a drag coefficient of 0.2 rather than 0.44 as assumed by Turner et al[25].

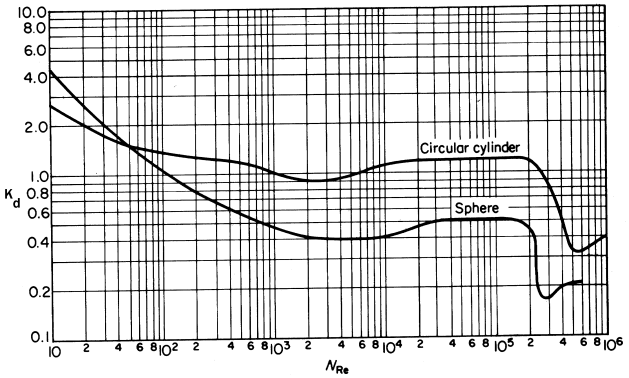

Figure 16 - Drag Coefficient for Spheres per Whitaker[30]

Inclined Flow Loop Experiments

Experimental Procedure

To investigate and determine the fraction of liquid that is unloaded, and the fraction of liquid that remains in a well during an off-bottom gas blowout at high gas velocities and at different angles of deviation from the vertical, an instrumented flow loop was used. The flow loop is comprised of two 48 ft pipes connected in a "U" shape. One side of the "U" contains the instrumented test sections and an inner short pipe fixed in a fully eccentric configuration at the top to simulate the off-bottom condition. The test loop can be inclined at any angle between 0 and 90 degrees from the vertical position. The test section is shown in Figure 17. The inside diameter of the outer pipe is 6.065 in., and the outside diameter of the inner pipe is 2.375 in. Five transducers are fixed to the flow loop to measure pressure, temperature and differential pressure at three locations. Two differential pressure cells provided liquid holdup for the off-bottom section, while the third differential pressure cell gave liquid holdup measurement in the annulus opposite the drillpipe. For the purpose of this study, only the readings of the differential pressure cells in the off-bottom condition were considered.

During the experiments, the liquid holdup was determined by means of the gas fraction for the two-phase flow applying the general energy equation, as suggested by Nakagawa[17]. For a given length of pipe test section, the total pressure change can be simply written as:

$$(dp)_{Tot} = (dp)_g + (dp)_f + (dp)_a \quad \ldots\ldots\ldots\ldots\ldots\ldots (17)$$

The term $(dp)_g$ accounts for the elevation change component, which relies on the liquid-gas mixture density. The term $(dp)_f$ accounts for the friction loss component which always causes a pressure drop in the direction of flow and is also a function of the liquid-gas mixture density and flow characteristics. The term $(dp)_a$ which accounts for the acceleration component, is the result of velocity changes during flow, and can be neglected for the low range of velocities of interest in these experiments. The term $(dp)_{Tot}$ is the total pressure drop, which can be measured directly by the differential pressure cells.

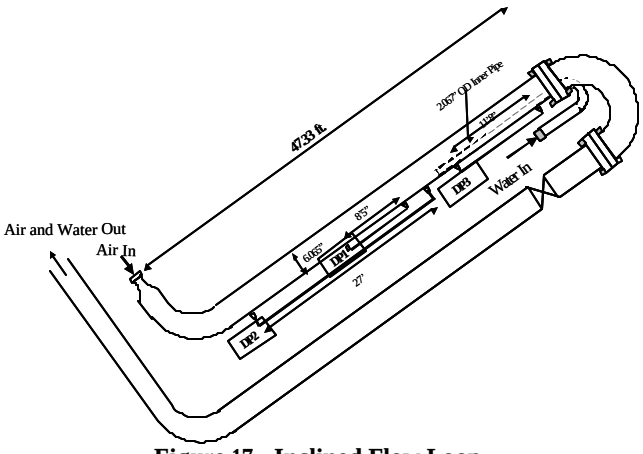

Figure 17 - Inclined Flow Loop

Solving Equation (17) for the liquid-gas mixture density, and knowing the density of the liquid and gas, the system can be solved to find the gas fraction and therefore the liquid holdup. This dynamic determination of liquid holdup was compared to the static, volumetric holdup that was trapped and measured in selected tests, with a very good agreement.

The experimental runs for each deviation angle started by loading the off-bottom section of the loop with liquid. Once the section was filled, and confirmed by the readings from the pressure

differential cells, air was injected at the bottom of the flow loop, at the lowest flow rate of the test matrix. Once the desired air injection rate was reached, and was flowing at a steady-state condition (which could be observed from the chart recorders), the data acquisition computer system recorded the selected parameters. Six to seven different air injection rates were performed for each test.

In order to reach high superficial gas velocities, the exit of the flow loop was vented to the atmosphere, resulting in pressures in the flow loop in the range of 16 to 22 psig, depending on the flow conditions.

Another experimental procedure was performed to directly measure liquid accumulation due to fallback. The air injection rate was established prior to the liquid injection. Then the liquid accumulation was assumed to have stabilized at a constant value when the desired air and liquid were flowing at a steady-state condition, and differential pressures had stabilized. The data acquisition computer system then recorded the desired parameters. The results showed that the same holdup is obtained at the same superficial gas velocities for both test procedures; therefore for operational simplicity, the first test procedure was chosen for subsequent tests. After a test was finished, the flow loop was moved to the next deviation angle to repeat the experimental procedure.

A schematic of the entire system for the inclined flow loop experiments is shown in Figure 18. The system includes a mud pit, centrifugal pump, air compressors and storage tank, and data collection system, as well as the flow loop and associated instrumentation.

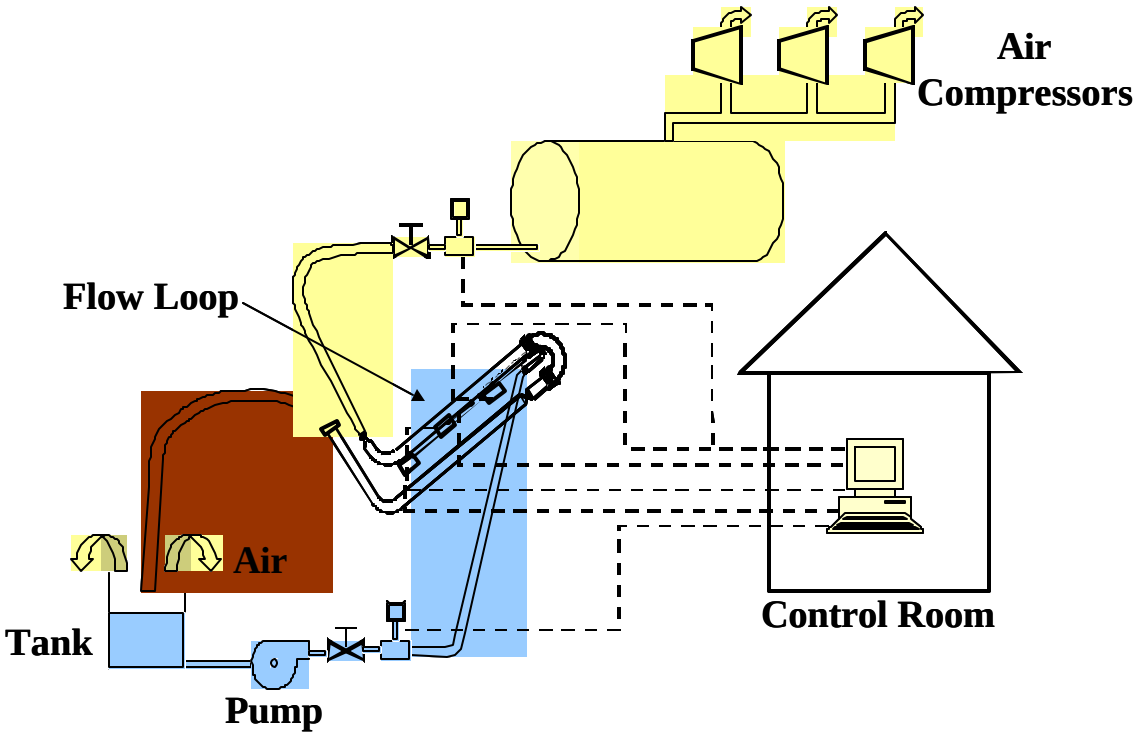

Figure 18 - Complete Experimental System for Inclined Flow Loop

Results

Experiments were performed with air as the blowout fluid and water, 10.5 ppg and 12.0 ppg mud as the kill fluid in the 48 ft flow loop at deviation angles of 0°, 20°, 40°, 60°, and 75° deviation angles from vertical.

The fluid properties used in these experiments are shown in Table 1. The formulations selected for the experiments were designed to both simulate real non-Newtonian fluids that might be used for well control operations and to give a significant range of densities and rheologies.

Figures 19 to 27 summarize the results of the tests performed in the experimental flow loop at the five different deviation angles considered of 0°, 20°, 40°, 60°, and 75° with the three different fluids. In these figures, WA denotes the tests performed with water, M1 denotes the tests made with 10.5 ppg mud, and M2 denotes the tests made with 12.0 ppg mud, followed by the angle at which each one was performed. The average superficial gas velocities for all angles, ranged from 0.34 m/sec to 12.61 m/sec. The ranges for the zero net liquid flow holdups for these angles were from 0.74 to 0.0, at the critical gas velocity. For the tests performed with water, in each test point there were two holdups obtained from the readings from the two different differential pressure cells for which values were very similar in all cases. The holdup considered representative for the results for this fluid was the simple average of these two readings.

Table 1 - Fluid Properties for the Experiment

Property	Water system	10.5 ppg system	12.0 ppg system
Density (ppg)	8.33	10.5	12
Plastic viscosity (cp)	1	17	23
Yield point (lbf/100sq ft)	---	14	21
Gel Strength – 10 sec. (lbf/100sq ft)	---	8	12

For the cases with the weighted mud (10.5 and 12.0 ppg), the readings from DP cell #1 showed the effect of mud contamination, meaning that the weighted mud was introduced into the tubing sensing the differential pressures in the DP cell, affecting the results and providing erroneous values. DP cell #2 provided a more reliable value that was confirmed by volumetric measurements after some tests. A complete table with all the data points can be found in Appendix B of the author's dissertation[5].

NOTE: continued on next page with Figure 19

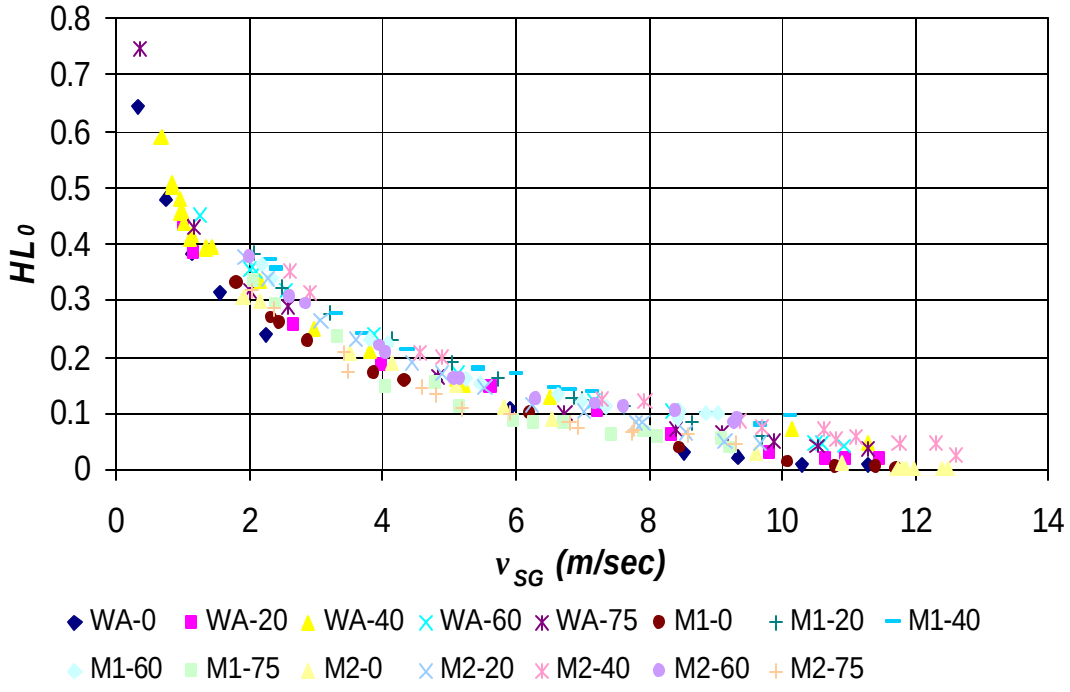

Figure 19 - Experimental results for All Angles and Fluids

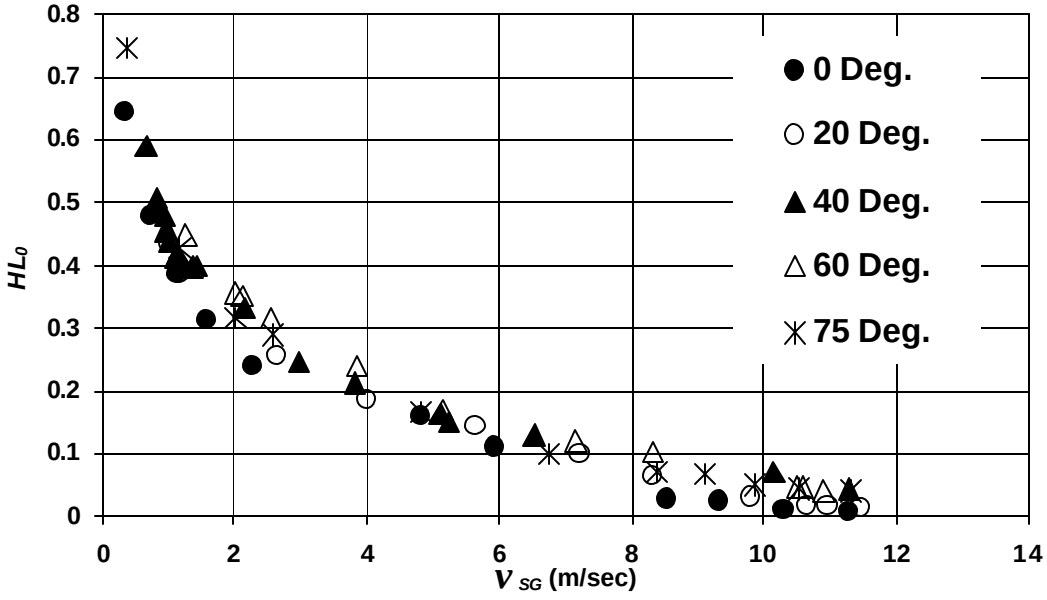

Figure 20 - Experimental results with Water at All Angles

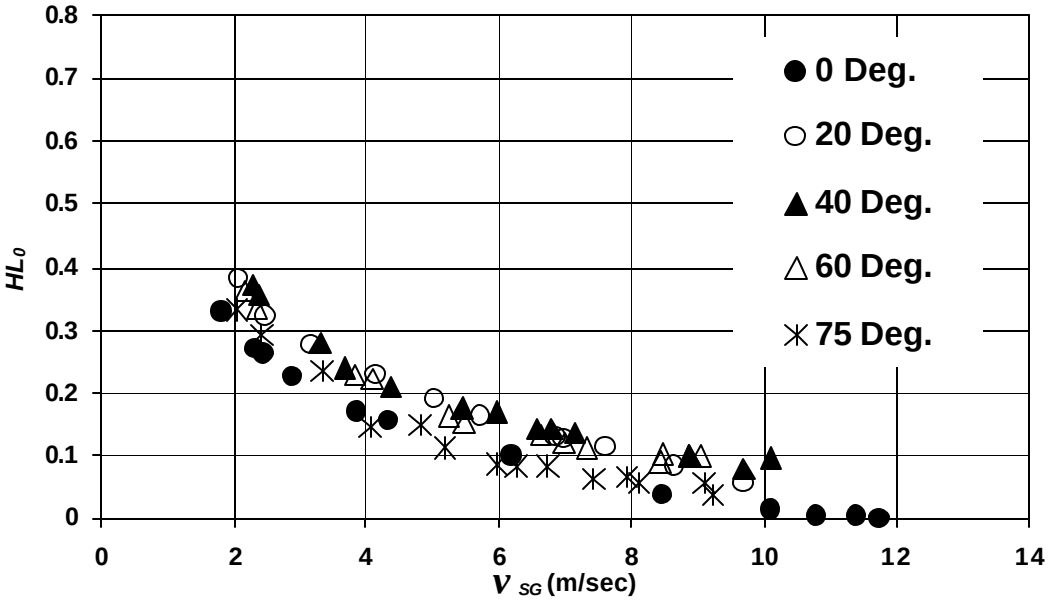

Figure 21 - Experimental results with 10.5 ppg Mud at All Angles

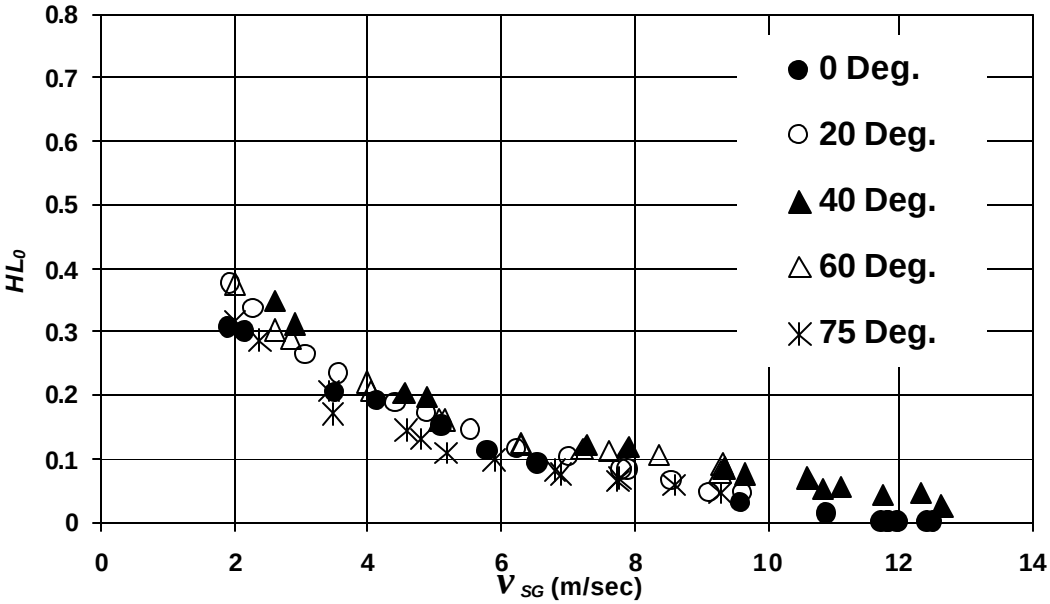

Figure 22 - Experimental results with 12.0 ppg Mud at All Angles

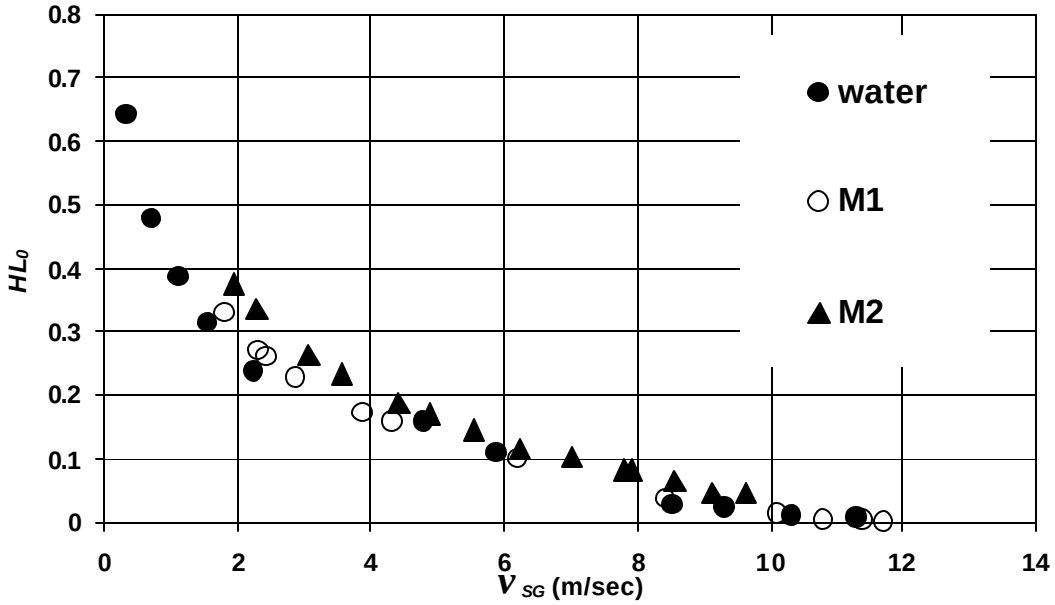

Figure 23 - Experimental results at 0 degrees Deviation (vertical) with the Three Fluids

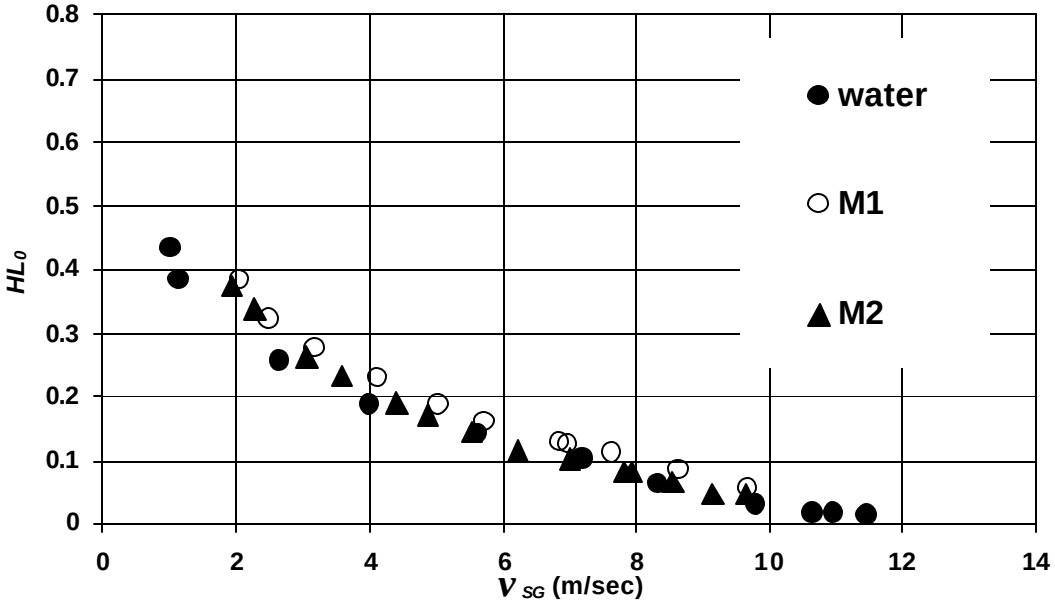

Figure 24 - Experimental results at 20 degrees Deviation with the Three Fluids

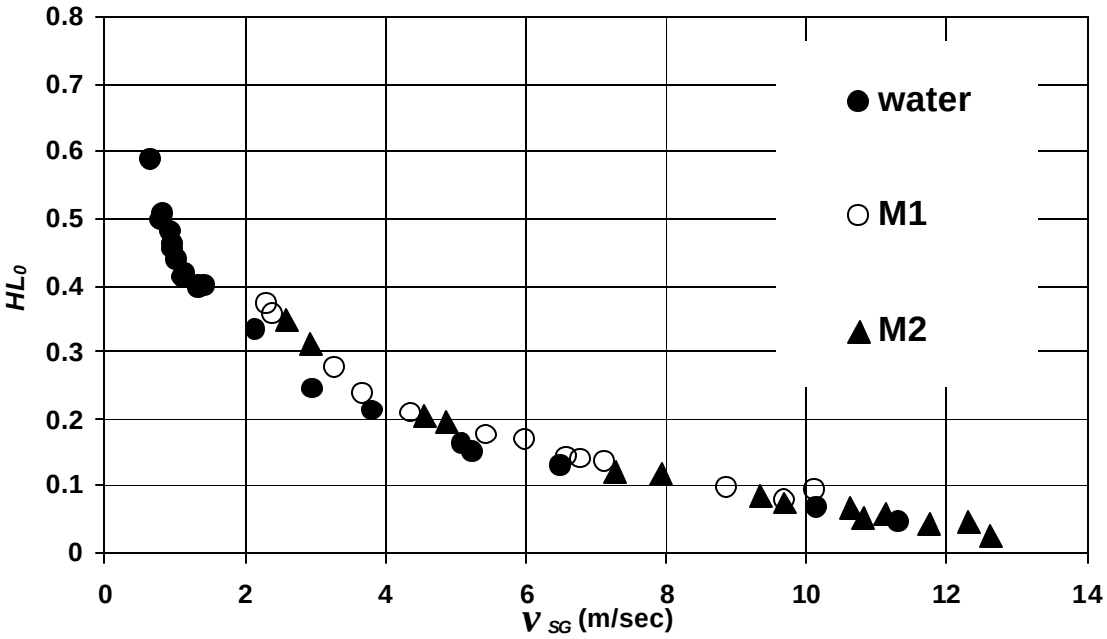

Figure 25 - Experimental results at 40 degrees Deviation with the Three Fluids

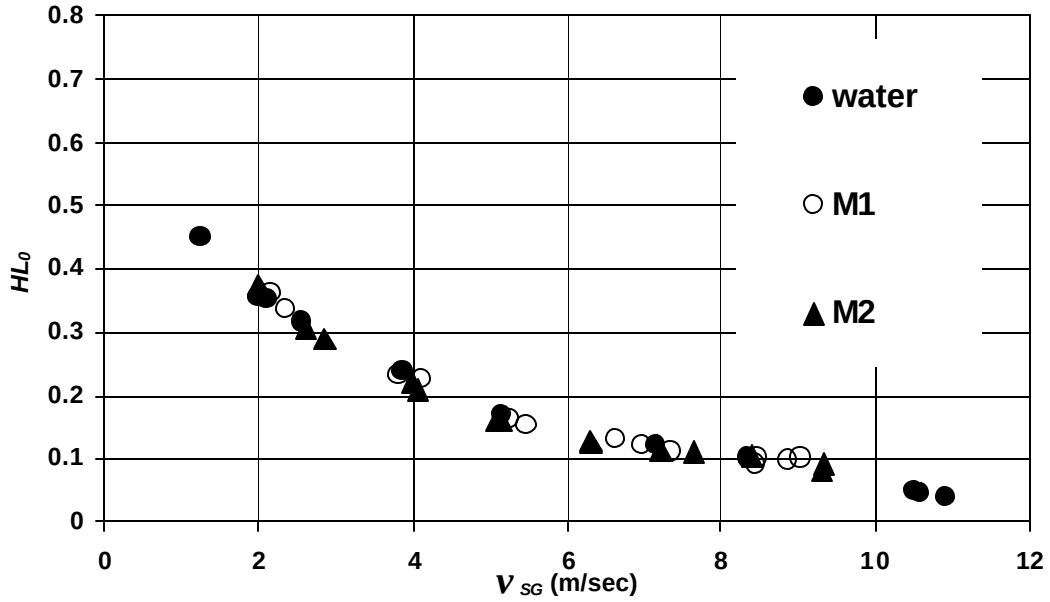

Figure 26 - Experimental results at 60 degrees Deviation with the Three Fluids

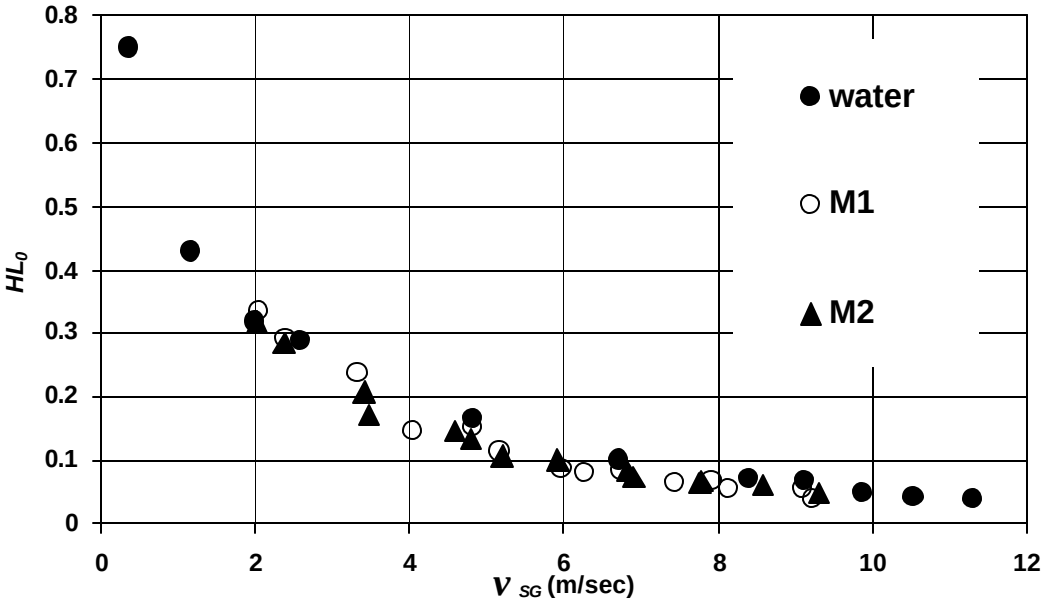

Figure 27 - Experimental results at 75 degrees Deviation with the Three Fluids

Analysis of Results

The critical air velocity for each experiment was based on the minimum velocity at which the observed liquid holdup was zero. If the critical velocity was not observed, it was estimated by extrapolating the liquid holdup to zero and determining the velocity at that point on the plot. An example of this extrapolation is shown for 10.5 ppg mud in an annulus at 20° inclination Figure 28.

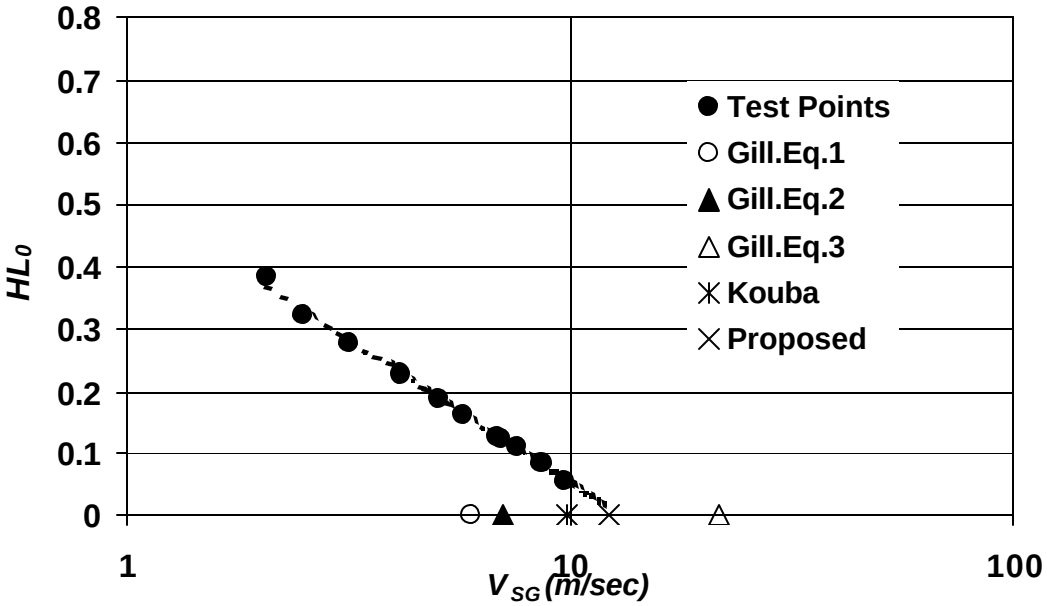

Figure 28 – ZNLF Holdup vs. Superficial Gas Velocity for 10.5 ppg Mud at 20 degrees Inclination

The zero net liquid flow holdup at each rate was determined as described in the previous section. This dynamic determination of liquid holdup was compared to the static, volumetric holdup that was trapped and measured in selected tests, with a very good agreement as shown in Table 2.

Table 2 - Comparison of Dynamic and Volumetric H_{L0}

Test	Water @ 0°	Water @ 40°	10.5 ppg mud @ 40°	12.0 ppg mud @ 20°	12.0 ppg mud @ 60°
H_{L0} Volumetric	.31	.44	.39	.35	.33
H_{L0} Dynamic	.30	.43	.37	.34	.30
Error (%)	3.2	2.3	5.1	2.8	9.1

The actual critical velocities determined in this manner were then compared with estimates of critical velocities calculated using the published methods reviewed earlier and the method proposed herein. Hypothetical critical velocities were calculated using the equations proposed by Gillespie[3], Equations (7), (8) and (9) for droplet diameter and (10) for the critical velocity. Kouba's Equation (14) was also used to calculate an estimate for critical velocity.

Finally the proposed method herein, Equation (16), was used to calculate the critical velocity using Turner's criteria with the proposed adaptation that defines the drag coefficient based on Figure 16. The deviation angle, flow conditions, velocity, and gas properties were used in determining the Reynolds Number and drag coefficient that correspond to the flowing conditions of the continuous phase. Tables 3 through 5 show the results of these calculations for the three different fluids. Using the proposed method, the Reynolds Numbers reached during the high velocity tests were in the highly turbulent region, corresponding to a drag coefficient of approximately 0.2, different from Turner's assumption of 0.44.

Table 3 – Calculated vs. Actual Critical Velocity for Water

Criteria	Reynolds No.	Calculated v_{Scrit} (m/sec)	Extrapolated v_{Scrit} (m/sec)	Difference (%)
Gillespie 1	22,922	5.55	11	49.5
Gillespie 2	37,759	6.60	11	40.0
Gillespie 3	8,361	20.75	11	88.6
Kouba	-------	9.14	11	16.9
Proposed 0° Dev.	487,625	11.13	11	1.2
Proposed 20° Dev.	495,267	11.31	11.5	1.7
Proposed 40°	521,222	11.90	12.5	4.8

Dev.				
Proposed 60° Dev.	579,887	13.24	13	1.8
Proposed 75° Dev.	683,655	15.61	12	30.1

The predicted v_{Scrit} for deviation angles from 0° up to 60° for the three different fluids, correspond well with a power-law extrapolation of ZNLF holdup to zero as in the example shown in Figure 28. The critical velocities calculated using the previously published criteria are also shown. As shown in Tables 3 to 5, the difference between the values of the extrapolated v_{Scrit} and that calculated with the proposed method is less than 7% in all these cases.

For the case of 75° deviation, as shown in Tables 3 to 5, the power law extrapolation of ZNLF holdup to zero does not show a good agreement with the proposed method. For angles greater than 60°, the theory of liquid droplets entrained in the high velocity gas core is probably no longer the mechanism that governs the process, yielding to inaccurate results. As previously observed by Bourgoyne et al[31], holdup at a given superficial gas velocity tends to be a maximum at a deviation angle from vertical of about 50°. In our case, the maximum holdup was observed to occur at about 60°. For this reason, it was considered that for deviation angles greater than 60°, and up to 75° which is the maximum in this study, the equivalent angle to be used in Equation (16) would be given by $\alpha_{equ}=120° - \alpha_{real}$. This proposed equation is just based on the symmetry that H_{L0} vs deviation angle curve shows, adjusting the results to the experimental data.

Table 4 – Calculated vs. Actual Critical Velocity for 10.5 ppg Mud

Criteria	Reynolds No.	Calculated v_{Scrit} (m/sec)	Extrapolated v_{Scrit} (m/sec)	Difference (%)
Gillespie 1	29,528	5.97	12	50.3
Gillespie 2	48,751	7.09	12	40.9
Gillespie 3	29,582	21.53	12	79.4
Kouba	-------	9.80	12	18.3
Proposed 0° Dev.	630,507	11.94	12	0.5
Proposed 20° Dev.	619,569	12.22	12.5	2.2
Proposed 40° Dev.	652,037	12.86	13.5	4.7
Proposed 60° Dev.	697,801	14.43	14.5	0.5

Proposed 75° Dev.	817,432	17.03	12	41.9

Table 5 – Calculated vs. Actual Critical Velocity for 12.0 ppg Mud

Criteria	Reynolds No.	Calculated v_{Scrit} (m/sec)	Extrapolated v_{Scrit} (m/sec)	Difference (%)
Gillespie 1	25,950	6.28	12	47.7
Gillespie 2	44,096	7.54	12	37.2
Gillespie 3	29,351	22.63	12	88.6
Kouba	-------	10.33	12	13.9
Proposed 0° Dev.	599,057	12.58	12	4.8
Proposed 20° Dev.	612,328	12.76	12	6.3
Proposed 40° Dev.	632,281	13.49	14	3.6
Proposed 60° Dev.	703,446	15.00	14.8	1.4
Proposed 75° Dev.	834,577	17.66	12.2	44.8

Under this assumption, the new v_{Scrit} for 75° for water is 12.14 m/sec, 13.25 m/sec for 10.5 ppg mud, and 13.74 m/sec for the 12.0 ppg mud. These new values show a good agreement with a power-law extrapolation of ZNLF holdup to zero with differences of 1.6%, 10.4% and 12.6% for each case.

Full-Scale Test Well Experiments

Experimental Procedure

An instrumented test well was used to investigate and determine the fraction of liquid that remains in a well during a gas blowout at high gas velocities in a realistic annular geometry as a means to determine the critical gas velocity. This vertical well is 2787 ft deep with 8 5/8 in casing and inner concentric tubings of 5 ½ in, 4 in x 2 7/8 in and 1.9 in hanging from the wellhead, see Figure 29.

Natural gas with 0.58 specific gravity was injected down the 1.9 in tubing, and circulated back to the surface up the 8 5/8 in x 5 ½ in annulus while monitoring bottom hole pressures through the static gas columns in the 4 in x 5 ½ in annulus and the 1.9 in x 4 in annulus. Seven tests were performed on this well, covering flow rates from 58,000 scf/hr up to 133,000 scf/hr.

Prior to the gas circulation, a known volume of drilling mud with 8.7 ppg density, plastic viscosity of 11 cp and yield point of 5 lbf/100ft², was placed in the 8 5/8 in x 5 ½ in annulus to be partially displaced by the gas, reaching a zero net liquid flow holdup at a particular steady state gas rate. Adjusting a choke downstream of the casing outlet from the well controlled the gas rate.

The recovered liquid at the surface was measured in a tank. The difference between the original known volume and the recovered volume was recorded as the remaining liquid volume in the well. The choke was then opened until a higher stabilized rate was achieved. The zero net liquid flow holdup was calculated as the ratio of the remaining liquid volume to total annulus volume. It is indicative of the fraction of the liquid or control fluid that will be accumulated in the well during flowing conditions.

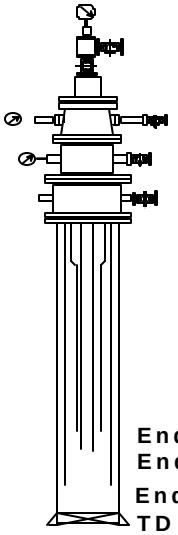

Figure 29 - LSU #1 Test Well

Results

Table 6 summarizes the results of the seven tests performed in the experimental well. Superficial gas velocities were calculated at average conditions between bottom hole and surface for each test. The average superficial gas velocities ranged from 0.59 m/sec to 4.83 m/sec. The corresponding zero net liquid flow holdups ranged from 0.45 to 0.046. Average pressures ranged from 698 psia to 209 psia.

Table 6 - Experimental Results in LSU Well #1

Q_g (scf/hr)	v_{SG}(m/sec)	Average Pressure (psia)	H_{Lo}
58,063	0.59	698	0.450
84,714	1.24	500	0.260
64,694	1.42	340	0.240
102,810	3.04	255	0.110
117,254	3.98	223	0.087
130,530	4.60	215	0.057
133,139	4.83	209	0.046

Analysis of Results

The method used for analyzing the full-scale well results was the same used for the flow loop experimental results. Table 7 shows the results of these calculations. Using the proposed method, the Reynolds numbers reached during the high velocity tests were in the highly turbulent region. As experienced in the flow loop experiments, these correspond to a drag coefficient of approximately 0.2, different from Turner's assumption of 0.44.

Table 7 - Calculated versus Actual Critical Velocity in LSU #1

Criteria	Reynolds No.	v_{Scrit} (m/sec)
Gillespie 1	37,022	2.83
Gillespie 2	43,460	3.01
Gillespie 3	26,458	10.96
Kouba	----	4.65
Proposed	317,798	5.66
Actual	----	5.99

The predicted v_{Scrit} of 5.66 m/sec corresponds well with actual critical velocity of about 5..99 m/sec given by a semi-log extrapolation of ZNLF holdup to zero as shown in Figures 30 and 31. This prediction is therefore more reliable for the test conditions than any of the methods proposed by Gillespie et al[3] or Kouba at al[26]. It also gives a predicted value similar to Turner et al's[25] recommended method using a drag coefficient of 0.44 and increasing v_{Scrit} by 20%. However the proposed method should be more reliable because it explicitly considers Reynold's number and the effect on drag coefficient.

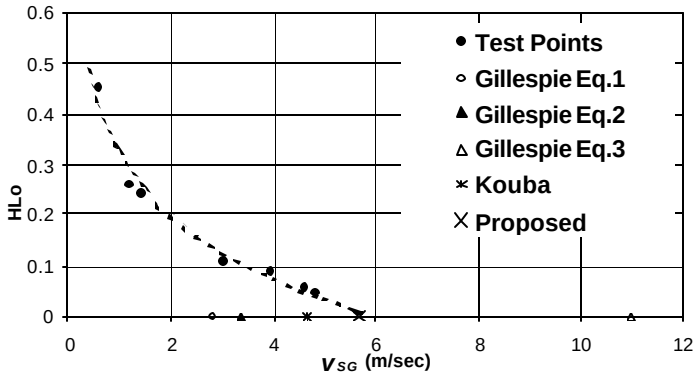

Figure 30 - ZNLF Holdup and v_{Scrit} for LSU #1

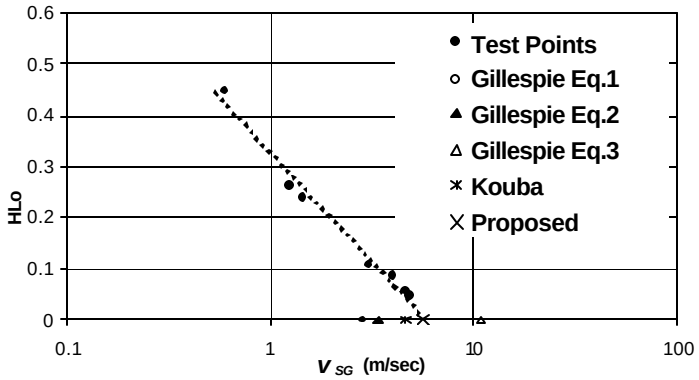

Figure 31 - ZNLF Holdup and v_{Scrit} for LSU #1 (semi-log)

Conclusions

1. Liquid holdups at high superficial gas velocities have been measured in a realistic annular geometry in a vertical research well using natural gas and water based drilling fluids

2. Liquid holdups at high superficial gas velocities and low pressure have been measured in an experimental flow loop at deviation angles from 0° to 75°, using an air and water system. These holdups correspond well to those measured in a realistic annular geometry in a vertical research well using natural gas and water based drilling fluids.

3. The critical velocity for complete kill liquid mud removal due to a blowout can be predicted by Equation (16). This modification of Turner's model of terminal velocity based on the liquid droplet theory, considers the deviation angle and the Reynolds number of the continuous phase when determining the drag coefficient. It gives more accurate predictions of critical velocity than any previously published method based on comparison to both flow loop and full-scale well experiments.

4. For deviation angles greater than 60° and up to 75°, using an equivalent angle equal to 120° minus the actual angle is suggested for use in Equation (16) to calculate critical velocity. This empirical correction currently has no theoretical basis but gives reasonable results for 75° inclinations.

Nomenclature

A_p Element area (ft^2)
d_i Pipe ID (ft)
d_{max} Maximum droplet size (ft)
F Factor to account for effect of turbulence on K_d
g Acceleration of gravity, 32.2 ft/sec^2

g_c	Critical acceleration of gravity, 32.2 lbm-ft/lbf-sec^2
H_{Lo}	ZNLF holdup.
K_d	Drag coefficient for spheres.
N_{Re}	Reynolds number.
p	Pressure (psia).
q_{gsc}	Gas flow rate at standard conditions (MMscf/D).
T	Temperature (? R)
$\overline{v}$	Average velocity of continuous phase (ft/sec).
v_s	Slip velocity (ft/sec).
v_{Scrit}	Critical gas velocity (ft/sec).
v_{SG}	Superficial gas velocity (ft/sec).
z	Gas compressibility factor at average pressure.
α	Deviation angle from vertical (Degrees)
α_{real}	Deviation angle from vertical (Degrees)
α_{equ}	Equivalent deviation angle from vertical (Degrees)
ρ_c	Density continuous phase (lbm/ft3).
ρ_d	Density disperse phase (lbm/ft3).
ρ_g	Gas density (lbm/ft3).
ρ_L	Liquid density (lbm/ft3).
σ	Surface tension (lbf/ft).
μ_c	Continuous phase viscosity (lbm/ft-sec).
μ_d	Disperse phase viscosity (lbm/ft-sec).

Chapter 5

Conclusions

Full-scale experiments were conducted to measure and model gas velocities and phase distributions during kicks and blowouts. Understanding these physical phenomena provides a basis for improving kick tolerance analysis and ultimately avoiding and controlling underground blowouts.

The two experimental subtasks of Task 7 have been completed and are described in this report. The experiments provided a reliable basis for estimating gas velocity and distribution during circulation of a kick and the critical gas velocity to unload all liquids from a well. A recap of the specific conclusions from those experimental studies is given herein.

1. Results of gas rise velocity obtained by previous researchers using flow tube data and the full scale experiments conducted as a part of this research are in close agreement. Equation (5) gives an appropriate estimate of gas rise velocity as a function of the mixture velocity.

2. Based on the experimental results, a simplified triangular gas distribution profile along the upward migration of the gas would be expected to provide further improvement in the accuracy of kick tolerance calculations.

3. The critical velocity for complete kill liquid mud removal due to a blowout can be predicted by Equation (16). This modification of Turner's model of terminal velocity based on the liquid droplet theory, considers the deviation angle and the Reynolds number of the continuous phase when determining the drag coefficient. It gives more accurate predictions of critical velocity than any previously published method based on comparison to both flow loop and full-scale well experiments. The effect of well deviation on the critical velocity was predicted based on balancing gravitational and drag forces for Equation (16). Estimated velocities are accurate up to an inclination of about 60°.

4. For deviation angles greater than 60° and up to 75°, using an equivalent angle equal to 120° minus the actual angle is suggested for use in Equation (16) to calculate critical velocity. This empirical correction currently has no theoretical basis but gives reasonable results for 75° inclinations.

Bibliography

1. Redman Jr., K. P. *"Understanding Kick Tolerance and Its Significance in Drilling Planning and Execution."* SPE Drilling Engineering, December 1991, pp. 245 - 249.
2. Wessel, M. and Tarr, B. A. *"Underground Flow Well Control: The Key to Drilling Low-Kick-Tolerance Wells Safely and Economically."* SPE Drilling Engineering, December 1991, pp. 250 - 256.
3. Gillespie, J. D.,Morgan, R. F., and Perkins, T. K., *"Study of the Potential for an Off-Bottom Dynamic Kill of Gas Well Having an Underground Blowout"*, SPE 17254, SPE Drilling Engineering, September 1990, pp. 215-219.
4. Ohara, Shiniti, *"Improved Method for Selecting Kick Tolerance During Deepwater Drilling Operations,"* Ph.D. Dissertation, Louisiana State University, May 1996.
5. Flores-Avila, Fernando Sebastian, *"Experimental Evaluation of Control Fluid Fallback during Off-bottom Well Control in Vertical and Deviated Wells,"* Ph.D. Dissertation, Louisiana State University, May 2002.
6. Flores-Avila, F. S., Smith, J. R., Bourgoyne, A. T., Bourgoyne, D. A., 2002, *"Experimental Evaluation of Control Fluid Fallback During Off-Bottom Well Control,"* Proceedings of the ETCE2002 Conference of ASME, Houston, TX, February 4-5, 2002, ETCE2002/DRILL-29030.
7. Flores-Avila, F. S., Smith, J. R., Bourgoyne, A. T., Bourgoyne, D. A., *"Experimental Evaluation of Control Fluid Fallback During Off-Bottom Well Control: Effect of Deviation Angle,"* Proceedings of the IADC/SPE Conference, Dallas, TX, February 26-28, 2002, SPE 74568.
8. Flores-Avila, F. S., Smith, J. R., Bourgoyne, A. T., *"New Dynamic Kill Procedure for Off-Bottom Blowout Wells Considering Counter-Current Flow of Kill Fluid,"* Proceedings of the SPE/IADC Middle East Drilling Technology Conference & Exhibition, Abu Dhabi, UAE, October 20-22, 2003, SPE/IADC 85292.
9. Baca, H. E., *"Co-Current and Counter-Current Gas Kick Migrations in High Angle Wells,"* MS Thesis, Louisiana State University, December 1998.
10. Baca, H., Nikitopoulos, D. E., Smith, J. R., and Bourgoyne, A. T., *"Co-current and Counter Current Migration of Gas Kicks in 'Horizontal' Wells,"* Journal of Energy Resources Technology, ASME, June 1999, pp. 96-101.
11. Baca, H., Nikitopoulos, D. E., Smith, J., and Bourgoyne, A. T., *"Counter-Current and Co-Current Gas Kicks in 'Horizontal' Wells: Non-Newtonian Rheology Effects,"* Journal of Energy Resources Technology, ASME, March 2003, pp. 51-60.
12. Ustun, Firat, *"The Effect of High Liquid Flow Rates on Co-Current and Counter-Current Gas Kick Migration in High Angle Wells,"* MS Thesis, Louisiana State University, December 2000.
13. Nakagawa, E. Y. and Lage, A. C. V. M. *"Kick and Blowout Control Developments for Deepwater Operations."* IADC/SPE 27497. IADC/SPE Drilling Conference, Dallas, TX, February 15 - 18, 1994.
14. Lage, A.C.V.M., Nakagawa, E. Y., and Cordovil, A.G.D.P. *"Experimental Tests for Gas Kick Migration Analysis*." SPE 26953, III SPE-LACPEC, Buenos Aires, Argentina, 1994.
15. Zuber, N., and Findlay, J. A. *"Average Volumetric Concentration In Two-Phase Flow System."* Journal of Heat Transfer, November 1965, pp. 453 - 468.
16. Johnson, A. B., and White, D. B. *"Gas Rise Velocities During Kicks."* SPE 20431. 65th Annual Technical Conference and Exhibition of Society of Petroleum Engineers, New Orleans, LA, September 23 - 26, 1990, pp. 295 - 304.

17. Nakagawa, E. Y. and Bourgoyne Jr., A. T.*"Experimental Study of Gas Slip Velocity and Liquid Holdup in an Eccentric Annulus."* Multiphase Flow in Wells and Pipelines, ASME - FED vol. 144, 1992, pp. 71- 79.
18. Mendes, P. P. M. *"Two-Phase Flow in Vertical and Inclined Eccentric Annuli."* MS Thesis, Louisiana State University, August 1992.
19. Wang, Y. *"Gas Slip Velocity through Water and Non-Newtonian Liquids in Vertical and Inclined Eccentric Annuli."* MS Thesis, Louisiana State University, December 1993.
20. Hinze, J. O., *"Critical Speeds and Sizes of Liquid Globules,"* Applied Scientific Research, Martinus Nijhoff, The Hague A-1, Mechanics, Heat, 1949, pp. 273-288.
21. Hanson, A. R., Domich, E. G. and Adams, H. S., *"Shock Tube Investigation of the Breakup of Drops by Air Blasts,"* Physics of Fluids Vol.6, No.8, 1963, pp. 1070-1080.
22. Karabelas, A. J., 1978, *"Droplet Size Spectra Generated in Turbulent Pipe Flow of Dilute Liquid/Liquid Dispersions,"* AIChEJ Journal, Vol.2, 1978, pp. 170-180.
23. Sleicher, C. A. Jr., *"Maximum Stable Drop Size in Turbulent Flow,"* AIChEJ Journal, Vol.8 No. 4, 1962, pp. 471-477.
24. Lopez, J. C. B. and Dukler, A. E., *"Droplet Dynamics in Vertical Gas-Liquid Annular Flow,"* AIChEJ Journal, Vol.33, No. 6, 1987, pp. 1013-1024.
25. Turner, R. G., Hubbard, M. G., and Dukler, A. E., *"Analysis and Prediction of Minimum Flow Rate for the Continuous Removal of Liquid from Gas Wells,"* J. Petroleum Tech., Vol.21, 1969, 1475-1482.
26. Kouba, G. E. MacDougall, G. R. and Schumacher, B. W., *"Advancements in Dynamic Kill Calculations for Blowout Wells,"* SPE 22559, SPE Drilling& Completion, September 1993, pp. 189-194.
27. Taitel, Y., Barnea, D., *"Counter Current Gas-Liquid Vertical Flow, Model for Flow Pattern and Pressure Drop,"* International Journal of Multiphase Flow, Vol.9, No. 6, 1983, pp. 637-647.
28. Coleman S. B., Clay, H. B., McCurdy, D. G., *"A New Look at Predicting Gas-Well Load-Up,"* J. Petroleum Tech., March 1991, pp. 329-333.
29. Nosseir, M. A., Darwich, T. A., Sayyouh, M. H., El Sallaly, M., *"A New Approach for Accurate Prediction of Loading in Gas Wells Under Different Flowing Conditions,"* SPE 66540, SPE Production & Facilities, 15 (4), November 2000, pp. 241-246.
30. Whitaker S., *"Introduction to Fluid Mechanics,"* second edition, Prentice-Hall, Inc., Englewood Cliffs, N.J., 1968, p. 305.
31. Bourgoyne, A.T., Wang Y., Bourgoyne, D.A., *"Experimental Study of Liquid Holdup During Well Unloading and During an Off-bottom Dynamic Kill,"* LSU/MMS well Control Workshop, Baton Rouge, Louisiana, March 30-31, 1994.

Appendix A

Improved Kick Tolerance Model for Deepwater Drilling Operations

This appendix contains a report presented by Shiniti Ohara and Adam T. Bourgoyne, Jr. to the LSU/MMS Well Control Workshop held in Baton Rouge, LA on May 23 and 24, 1995. The report describes the purpose of the research on gas distribution described in the main report in the context of a kick tolerance simulator developed by Mr. Ohara for PETROBRAS. The models forming the basis for the simulator are also described.

This report describes research towards an improved method for accurately estimating the maximum mud weight and hence the maximum depth that could be safely be drilled if well control operations became necessary on a floating drilling vessel operating in deep-water. The maximum mud density increase that can be handled without fracturing an exposed formation is called the kick tolerance of the well. As the kick tolerance decreases with increases in depth, the risk of formation fracturing during well control operations increases. Formation fracture often leads to an underground blowout that can be very expensive to control. Costs as high as $200,000,000 have been reported for control of a single underground blowout. In contrast, designing all deep-water wells with a high kick tolerance is quite expensive because of the large number of casing strings required. Another objective of this research is to develop appropriate criteria for evaluating risks and selecting appropriate values for minimum kick tolerance to be used in well design and while drilling.

An advanced kick simulator designed specifically for calculating kick tolerance for deep-water wells has been developed. The new software will also determine the kill capability (killable *kh* factor) of the available rig pumps.

Before an accurate kick tolerance simulator can be developed, experimental work is needed to determine the upward gas rise velocity and its distribution along the flow path during well control operations. The experiments (38 tests -- eight with water and 30 with drilling fluid) will be conducted in the LSU No. 2 well that has a special completion that permits simulation of the gas kick. The well will be monitored by superficial sensors and four downhole pressure sensors. The measured data will be used in modeling the gas rise velocity and gas concentration profile along the upward flow.

The availability of this simulator will result in improved well design, safer drilling operations, and improved capability for drilling in deeper water depths.

Introduction

Deep water drilling poses special problems such as low fracture gradients, high pressure loss in choke lines, overbalanced drilling due to a riser safety margin, generally high permeability formations, and emergency riser disconnection problems. As a result, new techniques and more reliable models must be developed to assist in well design criteria, kick detection, well control operations, and blowout contingency planning.

Key factor to successfully drilling deep-water wells are (a) a detailed well design and drilling plan and (b) close control while drilling to avoid kick, loss of circulation, and underground blowout. An underground blowout can be especially costly and is highly undesirable.

The kick tolerance concept has been shown to be a powerful tool that can be used during well design, along with the pore pressure and fracture gradients, to determine casing setting depths. In addition, kick tolerance can be used while drilling to estimate the fracture risk of the weakest exposed formation, if a kick was taken and circulated, that could lead to an underground blowout. Considering this parameter, the decision to anticipate the running of casing can be made. Furthermore, it can be a parameter of interest to governmental regulatory agencies, such as the Mineral Management Service in the US for regulating drilling activities.

Even though kick tolerance has been used in the drilling industry, the concept has been controversial[1]. Much confusion can be credited to the original definition: "difference between mud weight in use and formation pressure (expressed as mud weight equivalents) against which the well could be safely shut in without breaking down the weakest formation." For example, with a pressure integrity test at the casing shoe of 1.68 gr/cm^3 (14 lb/gal) and a mud density of 1.20 gr/cm^3 (10 lb/gal), many may consider that they are secure because they have a kick tolerance of 0.48 gr/cm^3 (4 lb/gal). This is only true if no influx (zero pit gain) occurs, but generally a kick is detected by the pit gain (increase of volume in the mud pits).

As a result, kick tolerance decreases as kick volume and depth increase. It is calculated assuming that natural gas (worst case) is the kick fluid. Also assumed is the maximum pit gain that would be expected before the blowout preventers are closed. The maximum pit gain used in the calculation is critical and must be appropriate for field operating practices, instrumentation, and rig crew training. Shut-in kick tolerance applies to well condition when the well is shut in. Circulating kick tolerance applies to the most severe conditions expected during the well control operations to remove the kick fluids from the well.

The circulating kick tolerance can easily be calculated as a simple model that assumes the influx of gas enters as a slug and remains as a slug during the circulation. This simple model, although easy to calculate, is very conservative if compared with a modern kick simulator as shown in Figure 1 (example of a deep water well in Brazil[2]).

In contrast, calculation of kick tolerance by existing kick simulators can be very time consuming. For example, it took almost one day to calculate five points to draw the upper curve in Figure 1. Although time consuming, using the kick simulators to calculate kick tolerance in this well saved around $100,000 in drilling costs. Thus, a less conservative, more realistic, reliable, faster kick simulator dedicated to calculate kick tolerance is desirable not only for use in well planning but also while drilling.

The determination of the gas rise velocity in annuli for various wells conditions is crucial and fundamental to the development of a more accurate kick tolerance calculation procedure. Despite many studies in this area with flow loops or a real well (using mud, Xantham gum, or water as a liquid phase and air, Nitrogen, or Argon gas as a gas phase), the necessary gas distribution profile still can not be reliably estimated. We now have some idea about the bubble front velocity, volume centered velocity, and the tail velocity, but how the shape of the distribution profile will change with time during the gas migration is unknown. Since the tail velocity is low, its volume along the well can be considerable. Consequently, experiments to determine these velocities and distribution profiles have to be done.

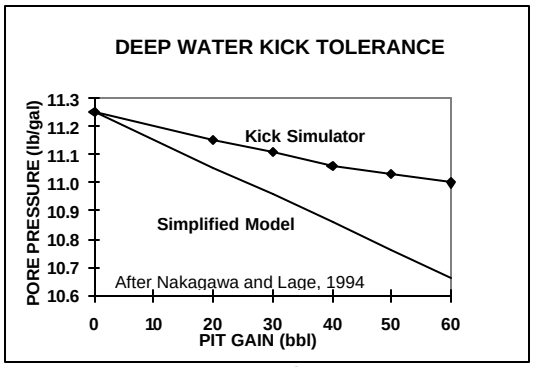

Figure 1 Kick Tolerance for Deep-water Well

The concept of kick tolerance is more complex in deep water drilling since dynamic position drilling ships (DPDS) are used, and normally a riser safety margin is applied to avoid an eventual loss of hydrostatic pressure due to an emergency disconnection and BOP failure. Depending on water depth, leak-off test results, and pore pressure the riser margin cannot always be applied because of the risk of formation fracture. The kick tolerance value can be near zero or even negative, without implying a dangerous situation, in this case.

Another important factor in deep-water is the high pressure loss in the long subsea flow lines. This factor has to be included in the kick simulator.

Under certain conditions, a greater risk of an underground blowout can be tolerated if it is known that control of the well could be regained using available rig equipment. The chance of being able to regain control of the well is estimated by calculating the product of permeability, *k*, and permeable zone thickness, *h*, which could be controlled using a dynamic kill procedure and the available rig pumps. The "killable *kh*" is routinely calculated by some operators[3,4] as drilling progresses. If it is determined that an underground blowout is not likely or that if one did occur it could be controlled with available rig equipment, a deeper casing setting depth may be selected. When the number of casing strings can be reduced, significant cost savings can be achieved without taking unacceptable risks of an underground blowout. One oil company[4] has successfully developed and applied the concept of killable kh when drilling multiple objectives under variant pore pressure conditions.

As a result, an advanced kick simulator that is dedicated to kick tolerance and killable *kh* calculations for deep water drilling is needed. It is important that the developed software be fast, reliable, and suitable for available rig site computers. Experiments have to be performed to determine the gas distribution profile in the annuli, and how the shape of the distribution profile will modify along the path of upward migration. In addition, the effect of high pressure losses in the kill line has to be incorporated into the model. Also the killable *kh* factor should be an output of the computer program.

Circulating Kick Tolerance Model

A mathematical model of a kick simulator dedicated to calculate the circulating kick tolerance is presented here. The proposed model is divided into submodels: a wellbore model, gas reservoir model, choke line model, and upward gas rise velocity model.

Wellbore Model

The wellbore unloading model includes the upward two-phase flow inside the annulus (well/drillstring, casing/drillstring, and riser/drillstring). This model was proposed by Nickens[5].

The model is based on: a) mass-balance equations (continuity equations) for the mud and gas, b) a momentum-balance equation for the gas-mud mixture, c) equation of state for mud and gas, and d) a correlation relating the gas velocity to the average mixture velocity plus the relative slip velocity between mud and gas to be determined in an experimental work.

Continuity Equations

The continuity equation is founded on the principle of mass conservation. Under unsteady two-phase flow conditions, the liquid phase continuity equation is given by:

$$\frac{\partial H}{\partial t} + \frac{\partial (v_l H)}{\partial z} = 0 \qquad (1)$$

where liquid holdup H is defined as:

$$H = \frac{\text{volume of liquid in an annular segment}}{\text{volume of annular segment}} \qquad (2)$$

and for the gas phase is given by:

$$\frac{\partial \left[\rho_g (1-H)\right]}{\partial t} + \partial \frac{\left[v_g \rho_g (1-H)\right]}{\partial z} = 0 \qquad (3)$$

Momentum Balance Equation

The momentum balance equation is based on Newton's second law of motion which states that the summation of all forces acting on a system is equal to the rate of change of momentum of that system. For two-phase flow the momentum balance equation is given by:

$$\frac{\partial \left[v_l \rho_l H + \left(v_g \rho_g (1-H)\right)\right]}{\partial t} + \frac{\partial \left[v_l^2 \rho_l H + \left(v_g^2 \rho_g (1-H)\right)\right]}{\partial z} + \frac{\partial p}{\partial z} + \left(\frac{\partial p}{\partial z}\right)_{elev} + \left(\frac{\partial p}{\partial z}\right)_{fric} = 0 \qquad (4)$$

where $(\partial p / \partial z)$ is the gradient pressure.

The elevation term or hydrostatic pressure gradient is given by:

$$\left(\frac{\partial p}{\partial z}\right)_{elev} = \frac{g}{g_c}\left[\rho_l H + \rho_g (1-H)\right] \qquad (5)$$

The friction term or frictional pressure gradient is calculated using the Beggs and Brill's[6] correlation modified for accounting the non-Newtonian characteristic of drilling fluids.

The two-phase flow friction factor f_{tp} is given by:

$$f_{tp} = f_F \cdot e^s \qquad (6)$$

where the no-slip friction factor f_F is obtained from a Fanning diagram (Craft et al[7]). The no-slip friction factor used by Beggs and Brill was for a smooth pipe curve on a Moody diagram.

The ratio of the two-phase slip to no-slip friction e^s is calculated as:

$$s = \frac{\ln \frac{l}{H^2}}{-0.0523 + 3.182 \ln\left(\frac{l}{H^2}\right) - 0.8725\left[\ln \frac{l}{H^2}\right]^2 + 0.01853\left[\ln \frac{l}{H^2}\right]^4} \qquad (7)$$

where the no-slip liquid holdup or input liquid content l is defined as:

$$l = \frac{q_l}{q_l + q_g} \qquad (8)$$

If l / H^2 is greater than 1.2 or less than 1.0 then the exponent s is calculated from:

$$s = \ln\left(2.2 \frac{l}{H^2} - 1.2\right) \qquad (9)$$

The frictional term is calculated from:

$$\left(\frac{\P p}{\P z}\right)_{fric} = \frac{f_{tp} r_{ns} v_m^{\ 2}}{2 g_c d} \qquad (10)$$

where the mixture velocity v_m is defined as:

$$v_m = v_l H + v_g (1 - H) \qquad (11)$$

and the two-phase no-slip density r_{ns} is defined as:

$$r_{ns} = r_l l + r_g (1 - l) \qquad (12)$$

Equation of State

Since in deep-water drilling only water-based mud is used, because of environmental pollution problems in case of an emergency disconnection of riser, the drilling fluid can be considered incompressible. Although Hoberock et al[8] showed that even in water-based mud the pressure and temperature can cause an error by hundreds of psi in deep wells when compared with the pressure calculated using constant surface densities. The reduction in bottom hole pressure for well depths up to 4,572 m (15,000 ft) is not so sensitive, and the mud density can be considered as incompressible in this study. In a case of deep-well drilling or if oil-based mud is used, effects of temperature and pressure should be considered (Ekwere et al[9]). Therefore, the density of mud is given by:

$$r_l = \text{constant} \qquad (13)$$

As for the gas density, a real gas equation of state is given by:

$$r_g = \frac{pM}{zRT} \qquad (14)$$

Gas Reservoir Model

Since little is primarily known about the properties of the gas reservoir during well design or while drilling, a detailed reservoir model is not usually justified.

Thomas et al (in Element et al[10]) introduced the use of equation:

$$q_{g_{sc}} = \frac{pkhT_{sc}}{(mzT)_f p_{sc} P_D}\left(p_f{}^2 - p_{bh}{}^2\right) \qquad (15)$$

where:

$$P_D = \frac{1}{2}\ln\left(t_D + 0.809\right) \qquad (16)$$

$$t_D = \frac{kt}{fm_f c_f r_w{}^2} \qquad (17)$$

The approximate solution (Equation 15) of the diffusivity equation requires the assumption of a constant gas flow rate. Since during a gas kick the bottom hole pressure and fluid flow rate vary, this assumption is not true.

Nickens made a slight modification in the Equation 15. He divided the gas formation into axial segments of thickness h_i equal to the rate of penetration (ROP) times the timestep in use. Then he considered that each segment flows independently of the other. As a result, the total gas-influx rate is then:

$$q_g = \sum_{i=0}^{N(t)} q_{gi} \qquad (18)$$

where $N(t)$ is the number of segments at time t. This modification to the flow equation removes the approximation that gas flow is axially symmetric within the exposed gas.

Implicit, also, is that the reservoir extends to infinity. In most kick control situation this assumption is acceptable because the gas flow time is short, and the reservoir boundary is not reached. In contrast, simulation of small pockets of gas is not allowed, but should not incur in a serious underground blowout.

Choke Line Model

A choke line is employed to carry fluids to the surface after the subsea blowout preventers (BOP) are closed. The long and narrow (3 in) choke line in deep-water leads to high velocity and consequently high pressure loss.

Elfaghi[11] did an experimental work using a full-scale model, at LSU, consisting of 914 m (3,000 ft) of 60 mm (2 3/8 in) subsurface choke line. For single phase mud flow, both the Bingham plastic and the power law non-Newtonian models provided acceptable comparison with observed data. For two-phase flow

through the choke line, Hagedorn and Brown[12] and Beggs and Brill correlations provided acceptable comparison with observed data. Therefore, the two-phase flow through choke line is considered the same as the annular flow.

Upward gas rise velocity model

The development of a reliable kick simulator needs an accurate model of gas-mud mixture flow as it moves upward in the wellbore. The empirical correlation relating the gas velocity to the average mixture velocity plus the relative slip velocity will be determined in an experimental work.

The Petroleum Engineering Department of Louisiana State University has been conducting a project in well control at the Petroleum Engineering Research and Technology Transfer Laboratory for more than a decade. Most of the experiments cited in this section were performed at this well facility.

Rader et al[13] verified that the assumption of gas flowing as a continuous slug and with the same velocity as the liquid did not work well when applied in a 1,828 m (6,000 ft) LSU research well. They observed lower gas velocity and lower casing pressure than expected during a well control operation.

When evaluating some kick control methods Matheus and Bourgoyne[14] reported the occurrence of bubble fragmentation. He observed that the bubble fragmentation is smaller in viscous fluids and less intense in the dynamic volumetric method.

Caetano[15] studied two-phase flow in a flow loop with flow of air-water and air-kerosene. He defined flow pattern maps for concentric and fully eccentric geometry. He concluded that the eccentricity affects the friction factor and the transition from bubble to slug flow. Furthermore, he proposed models for liquid hold up and pressure gradients for each flow pattern based on Taitel's[16] equations.

Motivated by the need for a better knowledge of bubble fragmentation process Bourgoyne and Casariego[17] made a theoretical and experimental study of gas kick in vertical wells. Their model closely predicated measured casing pressure with data from a 1,828 m (6,000 ft) LSU research well.

Rommetveit and Olsen[18] used an inclined (maximum of 63^0) research well to perform gas kick experiments using Nitrogen and Argon gas with oil-base mud. They used nine surface sensors to monitor the pump strokes, mud return flow rate, pit level, choke position, choke pressure, gas injection rate, choke line fluid density, standpipe pressure, and gas injection pressure. In addition, they used one hardwire sensor and four downhole memory tools to log the pressure and temperature. Based on the differential pressure among the sensors in the well and among the choke pressure and the sensors in the well they concluded that: a) the gas starts to dissolve immediately as it enters the wellbore; b) the bubble flow regime prevails in the two-phase section; c) the gas bubbles rise and dissolve; d) the initial gas-oil ratio (GOR) in the experiment was higher than the saturated GOR; e) gas bubbles rise and distribute over a longer section of the well; f) the gas dissolution is governed by convective diffusion, and the mud does not become saturated with gas immediately. They also observed some pulsations on the return flow, and their explanation was that gas bubbles first coalesce and form a slug of gas which rises fast and expands. After this a new dissolution process takes place in the upper part of the annulus.

Continuing a well control research at the LSU, Nakagawa and Bourgoyne[19] performed an experimental study in a fully eccentric flow loop at different inclinations to determine the gas fraction and gas velocity during the gas kick. They presented a simplified model for the gas-rise velocity eliminating the bubble size and shape for the calculation. Following this study, Mendes[20] and Wang[21] continued Nakagawa's experiments with lower superficial gas and liquid velocities which were not covered in previous experiments.

Using a flow loop, Johnson and White[22] performed some experiments to examine gas rise velocities during kicks. They used water and Xantham gum as a liquid phase and air as the gas phase. They concluded that in drilling fluids the bubbles rise faster than in water despite the increased viscosity. They explained that these surprising results are due to the change in the flow regime with large slug type bubbles forming at lower void fractions. Furthermore, their results show that a gas influx will rise faster than any previously published correlation would predict. One of their results, for vertical flow, is shown in a Zuber-Findlay[23] plot along with Nakagawa's, Mendes', and Wang's data in Figure 2. We can observe from this figure that Johnson's and Nakagawa's data are similar and can be fitted in a Zuber-Findlay correlation for the mean velocity of gas (v_g.)

$$v_g = C_0 v_m + v_s \qquad (19)$$

where the superficial mixture velocity (v_m) is defined as:

$$v_m = v_{gs} + v_{ls} = \frac{q_g + q_l}{A_{an}} \qquad (20)$$

Hovland and Rommetveit[24] experimented with gas kick in the same well used by Rommetveit and Olsen. In these experiments the authors used oil and water-based mud. The Nitrogen and Argon were injected to simulate the gas kick. They varied mud type, mud density, gas concentration, mud flow rates, and gas injection depth in their experiments. They concluded that in a high concentration gas kick, the gas rises faster than in low and medium concentration. The gas rise velocity correlations obtained from these experiments are not significantly dependent on gas void fraction, mud density, inclination, mud rheology, and surface tension. They presented one Zuber-Findlay plot, but the graphic had been normalized (divided by the maximum value). As a result, the experimental data cannot be compared with previous work.

Utilizing the same flow loop used by Johnson and White, Johnson and Cooper[25] investigated the effects of deviation and geometry on the gas migration velocity. For vertical orientation they concluded that the flow in the pipe and annulus are almost the same. The gas distribution coefficient (C_0) is the same while the gas slip velocity (v_s) is slightly larger in the annular geometry. In deviated flows C_0 is larger for the annulus and v_s is larger for the pipe. Up to a deviation of 45°, v_s remains almost constant. They also concluded that even in a stagnant mud, the gas normally migrates at a velocity over 0.5 m/s (5,900 ft/hr), almost six times the conventional field model of 0.085 m/s (1,000 ft/hr). The conventional field model considers only the hydrostatic effect of gas migration as:

$$\frac{dp_c}{dt} = \rho_m g v_s \qquad (21)$$

where dp_c/dt is shut-in pressure rise rate.

They used to calculate the gas rise velocity an equation developed by Johnson and Tarvin[26] to calculate the shut-in pressure rise rate (dp_c/dt):

$$\frac{dp_c}{dt} = \frac{X_k V_k \rho_m g v_s - q_e}{X_k V_k + X_w V_w + X_m V_m} \qquad (22)$$

Equation (22) considers the mud and wellbore compressibility and fluid loss into formation.

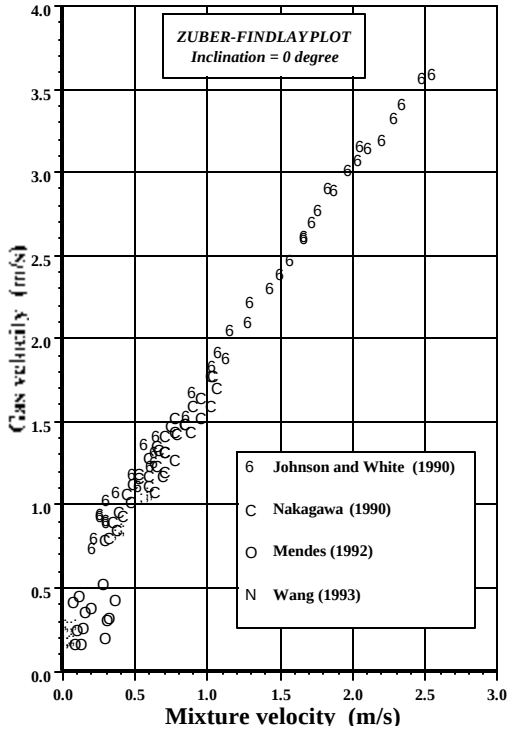

Figure 2 - Zuber-Findlay plot for flow-loop experiments

Lage et al[27] reported gas kick experiments performed in a 1,310 m (4,298 ft) vertical training well. The well has a 400 mm (13 3/8 in) casing set at 1,310 m and cemented up to surface. Inside this case, a 178 mm (7 in) casing, is placed to simulate the wellbore. A tubing of 48 mm (1.9 in) was used to inject the air at the bottom of the 178 mm casing passing through the annulus of 400 mm x 178 mm. In this same annulus an additional 48 mm tubing was placed at 800 m (2,625 ft) to simulate the casing shoe and circulation losses. Inside the 178 mm casing a drillstring composed with 121 mm (4 3/4 in) drill collars and 89 mm (3 1/2 in) drill pipes were run. A special sensor sub was made to accommodate the pressure sensor. Four sensors were placed at 302 m (991 ft), 600 m (1,968 ft), 877 m (2,877 ft), and 1,267 m (4,157 ft). Air and water were used in four tests. They measured three velocities: bubble front, volume centered, and bubble tail. If no gas is present between two sensors, the differential pressure is equal to hydrostatic pressure between them. The bubble front velocity can be measured dividing the distance between two upper sensors and the time elapsed between the beginning of differential pressure decrease in the two upper sensors and two lower sensors. Next, to measure the volume centered velocity they assumed that the center of the largest gas volume (when the differential pressure is minimum) is at the middle point of two sensors. They assumed that the air expansion and concentration changes are neglectable when the volume of air rise from the center of two lower sensors to the center of the pair above. Therefore, the volume centered velocity can be measured dividing the distance between the lower and upper pair of sensors and the time elapsed between the minimum differential pressure between the lower and upper pair of sensors. The tail velocity was measured considering the distance and differential pressure stabilization between two sensors. They observed that no significant difference was obtained among the velocities for open or shut-in well conditions. They obtained an average bubble front velocity of 0.26 m/s (3,070 ft/hr), an average tail velocity of 0.09 m/s (1,063 ft/hr), and an average volume centered velocity of 0.08 m/s (944 ft/hr) to 0.15 m/s (1,772 ft/hr). In addition, they derived an interactive equation for pressure build-up (choke pressure) prediction that fitted very well the data experiments:

$$p_c = \frac{1}{X_m}\ln\frac{V_w - V_k}{V_w + V_f - \frac{r_k V_k}{p_c}} \qquad (23)$$

Solution of the Differential Equations

The solution of differential equations is achieved using the numerical method of finite difference. This method was used by Nickens. There are many techniques to solve the differential equation by finite difference method. The "centered in distance and backward in time with a fixed space grid technique" was adopted in this study. The flow path is divided in a finite number of cells. Figure 3 shows a cell for two different time step.

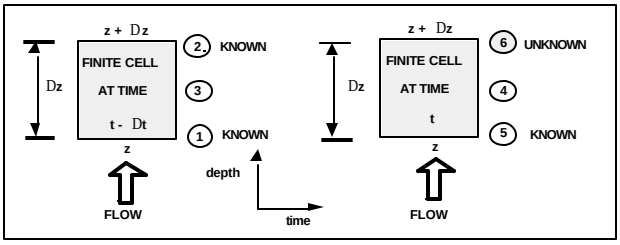

Figure 3 - Finite difference scheme for a cell

The finite difference formulation for the continuity equation in the space derivative is approximated by:

$$\frac{\partial U}{\partial z} = \frac{U_6 - U_5}{\Delta z} \qquad (24)$$

and the time derivative by:

$$\frac{\partial U}{\partial t} = \frac{U_4 - U_3}{t} = \frac{U_6 + U_5 - U_2 - U_1}{2\Delta t} \qquad (25)$$

where U is a function of z and t. Substituting these approximations into Equations (1) and (3), the finite difference formulation for the continuity equation for liquid became:

$$\frac{(v_l \rho_l H)_6 - (v_l \rho_l H)_5}{\Delta z} + \frac{(\rho_l H)_6 + (\rho_l H)_5 - (\rho_l H)_2 - (\rho_l H)_1}{2\Delta t} = 0 \qquad (26)$$

and for gas to:

$$\frac{\left[v_g \rho_g (1-H)\right]_6 - \left[v_g \rho_g (1-H)\right]_5}{\Delta z} + \frac{\left[\rho_g (1-H)\right]_6 + \left[\rho_g (1-H)\right]_5 - \left[\rho_g (1-H)\right]_2 - \left[\rho_g (1-H)\right]_1}{2\Delta t} = 0 \qquad (27)$$

The finite difference formulation for the momentum balance equation for the time derivative is the same as Equation (25), but the spatial derivative becomes:

$$\frac{\partial U}{\partial z} = \frac{U_6 + U_2 - U_5 - U_1}{2\Delta z} \qquad (28)$$

and substituting Equation (28) into Equation (4) gives:

$$\begin{aligned}
&\frac{1}{2\Delta z}\left\{\left[v_g^2 \rho_g (1-H)\right]_6 + \left[v_g^2 \rho_g (1-H)\right]_2 - \left[v_g^2 \rho_g (1-H)\right]_5 - \left[v_g^2 \rho_g (1-H)\right]_1 + \right. \\
&\left. + \left(v_l^2 \rho_l H\right)_6 + \left(v_l^2 \rho_l H\right)_2 - \left(v_l^2 \rho_l H\right)_5 - \left(v_l^2 \rho_l H\right)_1 \right\} + \frac{1}{2\Delta t}\left\{\left[v_g \rho_g (1-H)\right]_6 + \right. \\
&\left. + \left[v_g \rho_g (1-H)\right]_5 - \left[v_g \rho_g (1-H)\right]_2 - \left[v_g \rho_g (1-H)\right]_1 + \left(v_l \rho_l H\right)_6 + \left(v_l \rho_l H\right)_5 - \right. \\
&\left. - \left(v_l \rho_l H\right)_2 - \left(v_l \rho_l H\right)_1 \right\} - \frac{p_5 - p_6}{\Delta z} + \frac{1}{4}\left[\left(\frac{\Delta p}{\Delta z}\right)_1 + \left(\frac{\Delta p}{\Delta z}\right)_2 + \left(\frac{\Delta p}{\Delta z}\right)_5 + \left(\frac{\Delta p}{\Delta z}\right)_6\right]_{fric} - \\
&- \frac{1}{4}\left[\left(\frac{\Delta p}{\Delta z}\right)_1 + \left(\frac{\Delta p}{\Delta z}\right)_2 + \left(\frac{\Delta p}{\Delta z}\right)_5 + \left(\frac{\Delta p}{\Delta z}\right)_6\right]_{dev} = 0
\end{aligned} \qquad (29)$$

The calculation of the flow properties at point 6 in Figure 3 from those know properties at point 1, 2, and 5 require an iterative procedure. Points 1 and 2 represent the flow properties at the previous time step (t - Dt) in lower and upper boundaries respectively. Points 5 and 6 represent the same points as 1 and 2 but at the time step t. Points 3 and 4 represent arithmetic averaging at the center of the cell at t - Δt and t time steps, respectively.

The discretization procedure is only applied to the two-phase region. A single cell exists the first time, two cells for the second time and so on. The process for each time step starts in the top cell and ends in the bottom cell that coincides with the bottom hole of the well. Using this procedure the pressure at any given time step and position can be determined.

Experimental Program

The procedure for determination of upward gas rise velocity and distribution factor during well control operations is presented here.

Despite many studies in this area with flow loops and wells (using mud or Xantham gun as the liquid phase, and air, Nitrogen, or Argon gas as the gas phase), the necessary gas distribution profile still can not be reliably estimated. Furthermore, in the literature reviewed, we have not found an experiment that has used a full scale well with natural gas as a gas phase.

We now have some idea about the bubble front velocity, volume centered velocity, and the tail velocity. However, how the distribution profile will change with time during the upward gas migration is unknown. Since the tail velocity is low, its volume along the well, mainly in high viscosity mud, can be considerable.

Description of a full-scale well: LSU No. 2

The experiments will be carried out in the existing LSU No. 2 well, located at the Blowout Prevention Research Well Facility in Baton Rouge, Louisiana. The LSU No. 2 well is a vertical well which is 1,793 m (5,884 ft) deep and cased with 244 mm (9 5/8 in) casing. The well is completed with a 32 mm (1 1/4 in) gas injection line runs concentrically in a 89 mm (3 1/2 in) drilling fluid injection line. The well also contains 60

mm (2 3/8 in) perforated tubing which serves as a guide for well logging tools to be run in the annulus without risk of the logging cable wrapping around the drill string and becoming stuck.

Methodology of experiments

A drilling fluid composition matching those utilized to drill deep-water wells in the Campos Basin, offshore of Brazil, and natural gas will be utilized.

The gas will be injected at the desired injection rate through the 32 mm (1 1/4 in) tubing. Drilling fluid will be circulated down the annulus between the 89 mm (3 1/2 in) and 32 mm (1 1/4 in) tubings at the desired mud flow rate with returns taken from the 244 mm (9 5/8 in) casing.

During the experiments the drill pipe, casing and gas-injection pressures at the surface will be continuously monitored. The mud rate and the gas rate into and out of the well will be measured. One wired-to-surface downhole pressure sensor and three downhole pressures recording sensors will monitor the pressures developed during the well control experiments. A pressure signal will be generated at the beginning of the experiment to synchronize in time all four sensors. To investigate the concentration of gas in the tail of the multiphase region, samples of mud will be caught downstream of the separator after the major gas volume is circulated. The samples will then be analyzed to determine the concentration of the gas present in the mud.

Methodology to measure gas rise velocities

It is anticipated that the velocity of the kick front, velocity of the peak gas concentration, and the velocity of the tail of the two-phase region will be estimated through an analysis of the measured differential pressures. If no gas is present between two consecutive pressure sensors and mud is not being circulated, the differential pressure should reflect the hydrostatic pressure between them. When mud is being circulated, the differential pressure between two sensors should be equal to the sum of the hydrostatic pressure and the pressure losses between them.

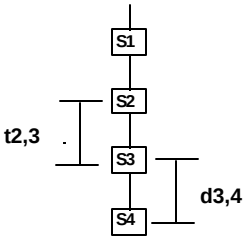

Figure 4 - Downhole pressure sensors disposition

When the gas front reaches each sensor, the differential pressure begins to decrease denoting the arrival of the bubble front. Thus, the velocity of the front can be estimated by dividing the distance between sensors by the elapsed time between the first arrival of the front. For example, from the Figure 4, the bubble front velocity between sensors 3 and 4 can be estimated knowing the distance $d_{3,4}$ and the time elapsed between the observed initial decrease in differential pressure between sensors 2,3 and sensors 3,4 using the following equation:

$$v_{front} = \frac{d_{3,4}}{\left(t_{2,3ini\Delta p} - t_{3,4ini\Delta p}\right)} \qquad (30)$$

Similarly, the tail velocity can be calculated as the distance between two sensors (for example, sensor 2 and 3) divided by the elapsed time to stabilize two adjacent differential pressures.

$$v_{tail} = \frac{d_{2,3}}{\left(t_{3,4\,stab\Delta p} - t_{2,3stab\Delta p}\right)} \qquad (31)$$

The study of the tail concentration with its lower velocity can show a large volume of gas inside the well that many previous investigators may have overlooked.

When the differential pressure between two sensors is a minimum, the largest amount of gas is present between the sensors, but the exact position of the peak concentration is not known. Therefore this should be investigated in this study. If it is assumed that the peak concentration occurs at the mid-point between two sensors, then the velocity of peak concentration can be computed as the distance between two mid points (e.g. between mid-point of sensors 3 and 4, and mid-point of sensors 2 and 3) divided by the elapsed time between them when the minimum values of differential pressure were recorded in the two adjacent well segments

$$v_{center} = \frac{\frac{d_{3,4}}{2} - \frac{d_{2,3}}{2}}{t_{4,3_{\min \Delta p}} - t_{2,3_{\min \Delta p}}} \qquad (32)$$

Since it will be possible to move the pressure sensors while the experiments are underway, it will be possible to verify if the above assumptions are justified. A more exact location of the peak concentration can be found by placing two pressure sensors closer together. After the peak concentration passes the location of the sensors, the sensors can be pulled to shallower depth to wait for the peak concentration to reach this new location.

After eight experiments with water and gas, thirty experiments are planned with drilling fluid and natural gas. The main parameters varied in the experiments will be gas injection rate, pit gain volume, mud circulation rate, and drilling fluid yield point.

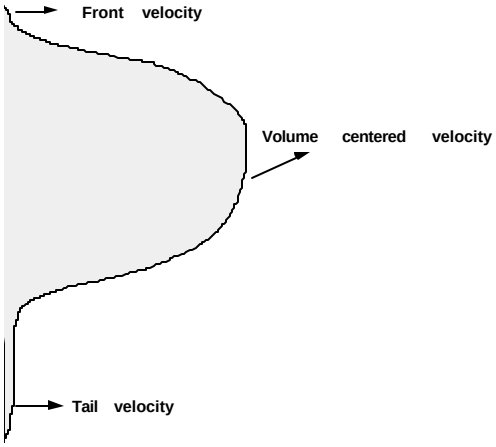

Figure 5 - Gas distribution profile

Gas Distribution Profile

Using the experimental data, we expect to determine how the shape and the gas distribution profile along the well will change with time during the upward flow. Since the tail velocity is low, if compared with the leading edge velocity or front velocity, its volume along the well can be considerable.

In a case that the gas distribution profile is successfully determined, the calculations for the kick simulator dedicated to calculate kick tolerance can be simplified.

Killable *kh*

Although an underground blowout is highly undesirable, for a hole section with a known but manageable underground flow potential, necessary unconventional well-control contingency plans can be developed. Wessel and Tarr[3] reported a new strategy to optimize well costs by managing the well-control risks better than an arbitrary minimum kick tolerance. A direct tradeoff exists between kick tolerance and well cost: specifying a higher kick tolerance than necessary can increase the well cost because additional casing strings will be required. Specifying lower kick tolerance can lead to costly well-control incidents. The authors first simplified the productivity index (J) as a function of only the product of the permeability (k) and the permeable zone thickness (h).

$$J = a\, k\, h \qquad (33)$$

By estimating the *kh* value for a potential gas zone to be drilled, one can determine whether an underground gas flow can be controlled with the available rig equipment or whether an additional pumping unit or a relief well will be required. Furthermore, neglecting the two-phase-flow liquid hold up and any friction pressure loss in the annulus, the kill-mud density and pump rate combination required to kill the underground flow is dependent on the volume of kill-mud available as shown in Figure 6.

Conclusion

Even though many experimental works, in full-scale wells, were accomplished, few results are published. None of the previous works had experiments in a combination of full-scale well and natural gas.

Moreover, the gas rises velocity and how the distribution profile varies with time are essential to the correlation of any kick simulator.

Kick tolerance concept has shown to be a powerful parameter to use in well design, during drilling, and for agencies that regulate the drilling activities. Therefore, kick tolerance should be used frequently, and its use should be facilitated by a computer program.

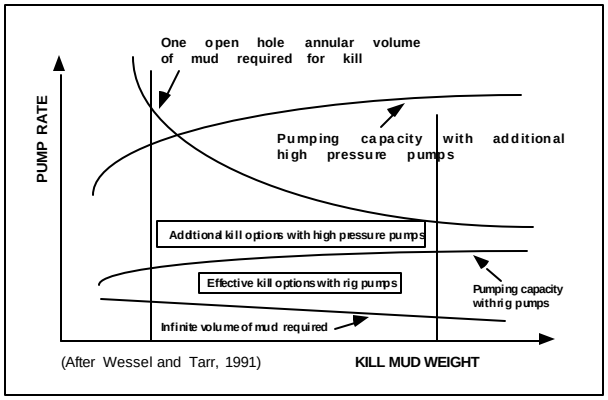

Figure 6 - Pump-rate requirements and equipment limits

Deep-water drilling and productions are reality today. Due to its intrinsic problems such as, low fracture gradients, high pressure loss in a long choke line, overbalanced drilling due to a riser safety margin, generally high permeability formations, and emergency riser disconnection problems new techniques or more reliable models must be developed to assist in well design criteria, kick detection, well control, and blowout contingency planning.

The availability of the kick simulator dedicated to calculate kick tolerance will result in improved drill planning, safer drilling operations, and improved capability for drilling in deeper water depths.

Acknowledgement

The authors would like to thank Petróleo Brasileiro S.A. (PETROBRÁS) for the financial support in this project and permission to publish this paper.

Nomenclature

Roman Letters

A_{an} = cross sectional area of annulus
c_f = formation compressibility
C_0 = gas distribution factor
d = distance
dp_c/dt = shut-in pressure raise rate (choke pressure)
e^s = ratio of the two-phase slip to no-slip friction factor

f_F = no-slip Fanning friction factor
f_{tp} = two-phase flow friction factor
g = gravitational acceleration
g_c = conversion factor
h = permeable zone thickness
H = liquid holdup
J = productivity index
k = permeability
M = gas molecular weight
p = pressure
p_{bh} = bottom-hole pressure
p_c = choke pressure
P_D = dimensionless pressure
p_f = formation pore pressure
p_{sc} = pressure at surface condition (standard condition)
q_e = average filtrate loss rate to formation
q_g = gas flow rate
q_{gsc}= gas flow rate at standard conditions
q_l = liquid flow rate
R = gas constant
r_w = wellbore radius
t = time
T = temperature
t_D = dimensionless time
T_{sc} = temperature at surface condition (standard condition)
v_{center} = volume centered gas velocity
V_f = fluid loss volume
v_{front} = gas front velocity
v_g = mean gas velocity
v_{gs} = superficial gas velocity
V_k = influx volume
v_l = liquid velocity
v_{ls} = superficial liquid velocity
v_m = mixture or homogeneous velocity
V_m = mud volume
v_s = slip velocity
v_{tail} = gas tail velocity
V_w = wellbore volume
X_k = influx compressibility
X_m = mud compressibility
X_w = wellbore elasticity
z = gas compressibility factor

Greek letters

α = constant
λ = no-slip liquid holdup or input liquid content
ϕ = formation porosity
μ = gas viscosity
μ_f = formation fluid viscosity
ρ_g = density of gas

ρ_l = density of liquid
ρ_m = density of drilling fluid or mud
ρ_{ns} = two-phase no-slip density
$\partial p / \partial z$ = gradient pressure
$(\partial p / \partial z)_{elev}$ = gradient pressure due to elevation
$(\partial p / \partial z)_{fric}$ = gradient pressure due to friction

Subscripts
ini = initial
Δp = differential pressure
min = minimum
sc = standard conditions
stab = stabilized

References

1. Redman Jr., K. P. *"Understanding Kick Tolerance and Its Significance in Drilling Planning and Execution."* SPE Drilling Engineering, December 1991, pp. 245 - 249.
2. Nakagawa, E. Y. and Lage, A. C. V. M. *"Kick and Blowout Control Developments for Deepwater Operations."* IADC/SPE 27497. IADC/SPE Drilling Conference, Dallas, TX, February 15 - 18, 1994.
3. Wessel, M. and Tarr, B. A. *"Underground Flow Well Control: The Key to Drilling Low-Kick-Tolerance Wells Safely and Economically."* SPE Drilling Engineering, December 1991, pp. 250 - 256.
4. Quitzav, R. and Muchtar, J. B., *"Drilling Safely at Well Design Limits: A Critical Well Design Case History*." IADC/SPE 23930. IADC/SPE Drilling Conference New Orleans, LA, February 18 - 21, 1992, pp. 749 - 754.
5. Nickens, H. V. *"A Dynamic Computer Model of a Kicking Well."* SPE Drilling Engineering, June 1987, pp. 159 - 173.
6. Beggs, H. D. and Brill, J. P. *"A Study of Two-Phase Flow in Inclined Pipes."* Journal of Petroleum Technology, May 1973, pp. 607 - 617.
7. Craft, B. C., Holden, W. R., and Graves, E. D. *"Well Design: Drilling and Production."* Prentice-Hall, Inc., 1962.
8. Hoberock, L. L., Thomas, D. C., and Nickens, H. V. *"Here's how compressibility and temperature affect bottom-hole mud pressure."* Oil and Gas Journal, March 22, 1982, pp. 159 - 164.
9. Ekwere, J. P., Chenevert, M. E., Zhang, C. *"A Model for Predicting the Density of Oil-Based Mud at High Pressures and Temperatures."* SPE Drilling Engineer, June 1990, pp. 141 - 148.
10. Element, D. J., Wickens, L. M., and Butland A. T. D. *"An Overview of Kicking Computer Models."* International Well Control Symposium/Workshop, Baton Rouge, LA, November 27 - 29, 1989.
11. Elfaghi, F. A. *"Pressure Losses in Subsea Choke Lines During Well Control Operations."* M.S. thesis, Louisiana State University, May 1982.
12. Hagedorn, A. R. and Brown, K. E. *"Experimental Study of Pressure Gradients Occurring During Continuous Two-Phase Flow in Small Diameter Vertical Conduits."* Journal of Petroleum Technology, April 1965.
13. Rader, D. W., Bourgoyne Jr., A. T., and Ward, R. H. *"Factors Affecting Bubble-Rise Velocity of Gas Kicks."* Journal of Petroleum Technology, May 1975, pp. 571 - 584.
14. Matheus, J. L., Bourgoyne Jr., A. T. *"Techniques for Handling Upward Migration of Gas Kicks in a Shut-In Well."* IADC/SPE 11376. IADC/SPE Drilling Conference, New Orleans, LA, February 20 - 23, 1983, pp. 159 - 170.
15. Caetano Filho, E. *"Upward Vertical Two-Phase Flow through an Annulus."* Ph.D. dissertation, The University of Tulsa, 1986.

16. Taitel, Y., Barnea, D., and Dukler, A. E. *"Modeling Flow Pattern Transitions for Steady Upward Gas-Liquid Flow in Vertical Tubes."* AIChEJ, 26(3), 1980, pp. 345 - 354.
17. Bourgoyne Jr., A. T. and Casariego, V. *"Generation, Migration, and Transportation of Gas-Contaminated Regions of Drilling Fluid."* SPE 18020. 63rd Annual Technical Conference and Exhibition of the Society of Petroleum Engineers, Houston, TX, October 2 - 5, 1988, pp. 19 - 28.
18. Rommetveit, R., and Olsen, T. L. *"Gas Kick-Experiments in Oil-Based Drilling Muds in a Full-Scale Inclined Research Well."* 64th Annual Technical Conference and Exhibition of the Society of Petroleum Engineers, San Antonio, TX, October 8 - 11, 1989, pp. 433 - 446.
19. Nakagawa, E. Y. and Bourgoyne Jr., A. T.*"Experimental Study of Gas Slip Velocity and Liquid Holdup in an Eccentric Annulus."* Multiphase Flow in Wells and Pipelines, ASME - FED vol. 144, 1992, pp. 71- 79.
20. Mendes, P. P. M. *"Two-Phase Flow in Vertical and Inclined Eccentric Annuli."* M.S. thesis, Louisiana State University, August 1992.
21. Wang, Y. *"Gas Slip Velocity through Water and Non-Newtonian Liquids in Vertical and Inclined Eccentric Annuli."* M.S. thesis, Louisiana State University, December 1993.
22. Johnson, A. B., and White, D. B. *"Gas Rise Velocities During Kicks."* SPE 20431. 65th Annual Technical Conference and Exhibition of Society of Petroleum Engineers, New Orleans, LA, September 23 - 26, 1990, pp. 295 - 304.
23. Zuber, N., and Findlay, J. A. *"Average Volumetric Concentration In Two-Phase Flow System."* Journal of Heat Transfer, November 1965, pp. 453 - 468.
24. Hovland, F. and Rommetveit, R. *"Analysis of Gas-Rise Velocities From Full-Scale Kick Experiments."* SPE 24580. 67th Annual Technical Conference and Exhibition of Society of Petroleum Engineers, Washington DC, October 4 - 7, 1992, pp. 331 - 340.
25. Johnson, A. B., and Cooper, S. *"Gas Migration Velocities During Gas Kicks in Deviated Wells."* SPE 26331. 68th Annual Technical Conference and Exhibition of the Society of Petroleum Engineers, Houston, TX, October 3 - 6, 1993, pp. 177 - 185.
26. Johnson, A. B. and Tarvin, J. A. *"Field calculations underestimate gas migration velocities."* IADC European Well Control Conference, 1993.
27. Lage, A.C.V.M., Nakagawa, E. Y., and Cordovil, A.G.D.P. *"Experimental Tests for Gas Kick Migration Analysis."* SPE 26953, III SPE-LACPEC, Buenos Aires, Argentina, 1994.